Journal of
Composites Science

MDPI

Review

An Overview of Recent Advancements in Conducting Polymer–Metal Oxide Nanocomposites for Supercapacitor Application

Pranoti H. Patil †, Vidya V. Kulkarni † and Sushilkumar A. Jadhav *

School of Nanoscience and Technology, Shivaji University Kolhapur, Vidyanagar, Kolhapur 416004, India
* Correspondence: sushil.unige@gmail.com; Tel.: +91-0231-260-9000
† These authors contributed equally to this work.

Abstract: Supercapacitors have gained significant attention as energy storage devices due to their high specific power, fast charge–discharge rate and extended cycling stability. Recent research focuses on the search for new electrode materials to enhance the specific capacitance of supercapacitors. Conducting polymers (CPs) and metal oxides (MOs) are being extensively tested as electrode materials in supercapacitors. CPs have poor cycling stability and low mechanical strength but are easy to process, while MOs exhibit easy availability, variable oxidation states and possess high specific capacitance, but they are somewhat difficult to process. Therefore, combining both (CP) and (MO) in a composite offers better results for the electrochemical performance of supercapacitors. This review mainly focuses on the discussion of CP/MO based nanocomposites recently reported for supercapacitor applications. The collective information presented in this report will provide researchers a view into the latest developments in this field. The continued research on this topic will reveal further potential applications of CP/MO composites.

Keywords: conducting polymers; metal oxides; nanocomposites; supercapacitor

check for updates

Citation: Patil, P.H.; Kulkarni, V.V.; Jadhav, S.A. An Overview of Recent Advancements in Conducting Polymer–Metal Oxide Nanocomposites for Supercapacitor Application. *J. Compos. Sci.* **2022**, *6*, 363. https://doi.org/10.3390/jcs6120363

Academic Editor: Francesco Tornabene

Received: 17 October 2022
Accepted: 23 November 2022
Published: 1 December 2022

Publisher's Note: MDPI stays neutral with regard to jurisdictional claims in published maps and institutional affiliations.

Copyright: © 2022 by the authors. Licensee MDPI, Basel, Switzerland. This article is an open access article distributed under the terms and conditions of the Creative Commons Attribution (CC BY) license (https://creativecommons.org/licenses/by/4.0/).

1. Introduction

Energy has become a significant focus of research for sustainable development in the global context. The development and refinement of more efficient energy storage devices or systems has become the need of the hour. To fulfil the growing demand for sustainable and renewable power sources, steps have been taken to manufacture flexible, lightweight and environmentally friendly energy storage systems. Therefore, recent research focuses on energy storage systems that are efficient, cleaner, and that can meet current energy needs [1]. An energy storage device should fulfil the desired requirements specific to high energy density (Wh), power (W), portable size, light weight, low cost, high shelf life etc. [2–5]. Various energy storage and conversion devices are being studied; of these, the supercapacitor has qualified to be one of the most potent devices for storing electrical energy [6]. Supercapacitors are designed to bridge the gap between batteries and capacitors to form fast-charging energy storage devices of intermediate specific energy [7,8]. Supercapacitors have shown their application in hybrid electric vehicles, load cranes, military field, integrated grid, portable electronic devices such as digital cameras, mobile phones, etc. [9–11]. They are known to work in conjunction with other energy storage (and producing) devices such as batteries and fuel cells [12]. Supercapacitors are favoured over batteries when high-power density, quick charge–discharge rates, longer life cycles and superior reversibility are necessary [13–16]. Supercapacitors are classified into three main types, electric double-layer capacitor (EDLC), pseudocapacitor and hybrid as represented in Figure 1. In the EDLC, the charge storage mechanism takes place at the interface between the electrode of the capacitor and the electrolyte solution. The electrode materials in EDLC are carbon foam, carbon aerogels, carbide-derived carbon (CDC), graphene, carbon

nanotubes (CNT's) and activated carbon (AC). In pseudocapacitors, the charge storage mechanism involves a Faraday reaction on the surface of the electroactive material on the electrode. Here, CPs and MOs are used as electrodes. The hybrid supercapacitor, by its name, involves working with both EDLCs and pseudocapacitors. It includes three types, namely asymmetric pseudo/EDLCs, composites and rechargeable battery types [1,17,18].

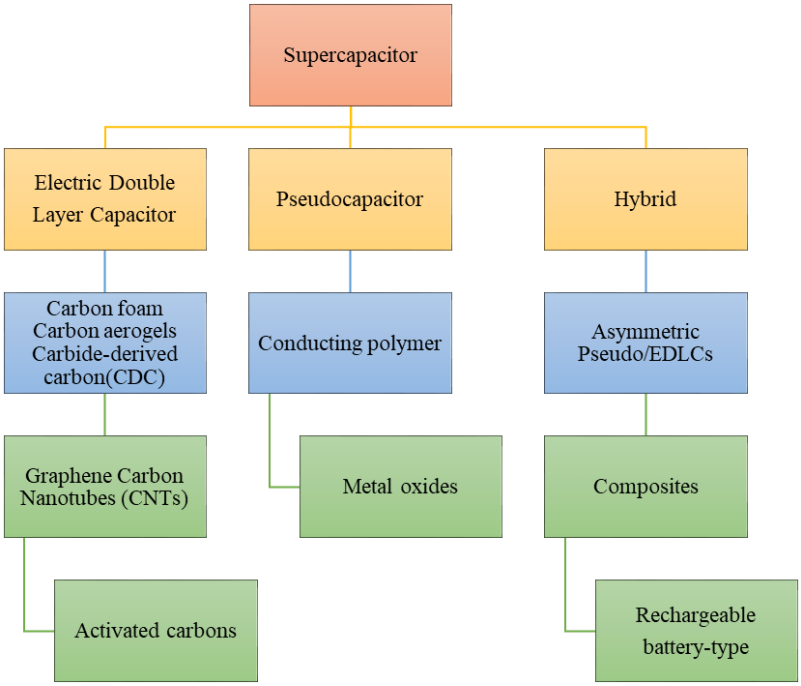

Figure 1. Types of supercapacitors.

A huge number of reports appear in the literature about the development of newer materials to be used as electroactive materials in supercapacitors. The materials are of various types, such as different carbon materials, mixed metal oxides, or composites comprising both these materials. The domain of CP–MO-based materials has also increased drastically where binary or ternary composites made from different CPs and MOs are reported for supercapacitor application. This literature review is primarily concerned with current advancement in CP–MO-based nanocomposites as materials for supercapacitor electrodes. First, we examine different conducting polymers, their characteristic, and the domains in which they are used. Second, we examine various metal oxides and their uses in supercapacitor applications. Then, we emphasize the advancements made possible by using CP–MO nanocomposites in supercapacitor applications. The evaluation concludes with some future perspectives.

2. Conducting Polymers

CPs are gaining significant attention due to their broad level of electrical conductivity, thermal stability, processability and mechanical flexibility [19]. Polymers that are intrinsically conducting were discovered several years ago, catching the attention of scientists due to their numerous applications in many sectors [20]. Due to their electrical conductivity values comparable to that of metals, they are also known as synthetic metals [21]. Three collaborating scientists MacDiarmid, Shirakawa and Heeger played a major role in enhancing the semiconducting behaviour of organic CPs (namely polyacetylene, which was synthesized through chemical polymerization). In 2000, these three researchers were awarded the Nobel Prize in Chemistry for inventing CPs [22]. This was a milestone moment, as it established a new field of research in the zone of chemistry and material science, as well as opening the path for new opportunities. The revelation by Heeger and MacDiarmid that oxidative doping could boost the polymer's conductivity by several orders of magni-

tude sent shockwaves across the polymer and electrochemistry worlds. This influenced a search for new CPs. The goal was to develop an organic polymer that could enhance the electric conductivity by doping so that it could compete with the electrical qualities of a metal [23]. Electrical CPs include polyacetylene (PA), polypyrrole (PPy), polyaniline (PANI), polythiophene (PTh), etc. [24,25]. CPs have attracted considerable attention due to their properties of high pseudocapacitance, conductivity, and ease of manufacturing and processing. However, they suffer from a transient cycle life and have poor mechanical properties [26,27]. Examples of CPs and their structures are shown in Figure 2 [19,28–30].

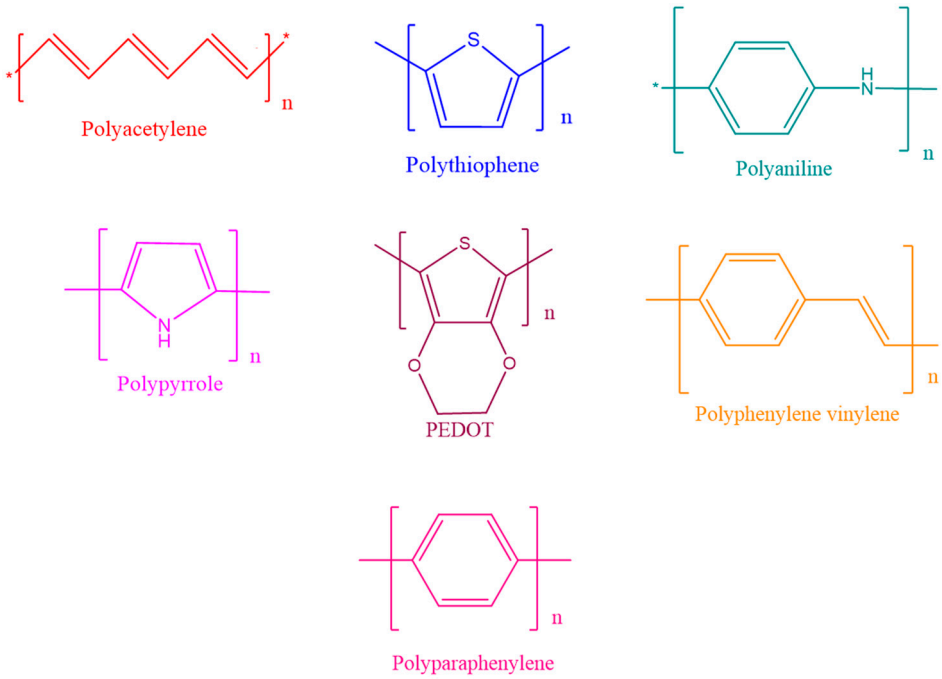

Figure 2. Structures of some common conducting polymers.

Brief information about each conducting polymer is provided below:

Polyacetylene (PA)

PA is the first organic polymer with the potential to conduct electricity that has enabled the use of organic compounds in electronics. It is a linear polymer comprising alternate carbon–carbon double bonds. The behaviour of PA and its derivatives is multifunctional. Some of its characteristics include electric conductivity, photoconductivity, liquid crystal qualities and chiral recognition. The conductivity of PA is in the range of 10^{-5} Scm^{-1}, which can be enhanced up to 100 to 1000 Scm^{-1} by doping. P-doped PAs are prepared from halogen derivatives [19,23,25].

Polythiophene (PTh)

The structures of PPy and PTh are very close to each other; the only difference is the hetero-atom. PTh has a sulphur atom instead of a nitrogen atom in PPy and a conjugated double bond in its polymer backbone. The band gap of PTh is low. PTh is a widely studied CP due to its strong electrical conductivity, optical characteristics, low cost and environmental stability. Electrical supercapacitors, non-linear optics, polymer light-emitting diodes (PLEDs), electrochromic, photoresists, antistatic coatings, sensors, batteries, magnetic-shielding materials, solar cells, memory devices, transistors, and imaging materials are all made from PTh [31,32].

Polyaniline (PANI)

Polyaniline, frequently abbreviated as PANI, is also sometimes referred as aniline black because of its dark pigment colour. PANI is a CP consisting of benzoid and quinoid rings. It exists in three forms according to their oxidation states, namely leucomeraldine (fully reduced), which consists of a benzoid ring; pernigraniline (fully oxidized), which consists

of a quinoid ring; and emeraldine (partially oxidized and partially reduced), consisting of a benzoid and quinoid ring. Out of these three forms, both leucomeraldine and pernigraniline are non-conducting, while emeraldine is conducting. Doping increases the electric conductivity of PANI. Dopant material reduces the band gap of PANI, which enriches electric conductivity. Being lightweight, less toxic, environmentally friendly, flexible, cost effective, delivering good electrical conductivity and showing thermal stability, PANI is a crucial CP in pseudocapacitor materials for electrochemical energy storage [19,26,33–36].

Polypyrrole (PPy)

PPy is a long-conjugated polymer comprising pyrrole as a monomer in quinoid form, which conducts electricity when it is oxidized and shows amorphous behaviour, but 15% crystallinity is shown by bulk PPy. PPy is a frequently studied CP comparable to many others because of its uncomplicated synthesis, stability in oxidised form, greater electrical conductivity and favourable redox properties. It is one of the most promising p-type CPs for the faradaic pseudocapacitor application because of its distinctive qualities, including strong conductivity, a quick charge–discharge mechanism, good thermal stability, low cost and high energy density [19,37].

Poly (3,4-ethylenedioxythiophene) (PEDOT)

The monomer of PEDOT CP is 3,4-ethylenedioxylthiophene. It is a major polythiophene derivative mainly researched for its high electrical and electro-optical properties. It also has numerous benefits, such as good conductivity, stability, as well as transparency. Its major disadvantage is poor solubility in water; however, this can be controlled with the addition of polystyrene sulphonate (PSS), which acts as both a dopant and a stabilizer. PEDOT is utilised in many different applications, including printed electronics, capacitors, touch screens, organic solar cells, organic light-emitting diodes, and antistatic [19,25,38,39].

Poly (paraphenylene vinylene) (PPV)

PPV is a highly crystalline polymer that possesses high mechanical strength and environmental stability. It has a low conductivity of about 10^{-13} Scm^{-1}, which can be extended up-to 1000 Scm^{-1} by doping with iodine, ferric chloride and alkali metals. As a result of its high optical property, PPV was the first electroluminescent material used to create organic light-emitting diodes (LEDs). It was widely researched for the production of LED displays and has scope in the field of optoelectronics [19,25].

Poly (para phenylene) (PPP)

PPP is a polymer made of repeating units of paraphenylene, in which benzoid rings are directly linked by C-C bonds. When doped, its conductivity increases several times. PPP has received significant attention because of its high thermal stability, high air stability, easy doping and tuneable conduction properties. Its high optical property plays an important role in manufacturing organic LEDs [19,25]. The range of the conductivity values and advantages of some CPs are mentioned below in Table 1 [40].

CPs have gained attention in the scientific world because of their remarkable characteristics, such as tuneable electrical conductivity, an easy method of synthesis, light weight [41], high optical qualities, efficient mechanical properties, effective microwave absorption properties, etc. [19]. They also exhibit properties such as anti-corrosion, as well as catalytic properties. CPs have led their application as a material for electrode in supercapacitors, Li-ion battery, and as an electrocatalyst and energy transfer mediators in solar cells and fuel cells [20]. They have also found application in data storage systems, transistors and switches, etc. [42]. These applications are summarized in Figure 3 [20,42]. Although CPs have a greater number of advantages, they are not good materials for use as electrodes for supercapacitors. Researchers have attempted to understand the CP-based electrochemical stability and performance of supercapacitors in order to create binary as well as ternary composites [43]. Therefore, CPs are normally mixed with MOs to obtain efficient electroactive materials.

Table 1. Bulk properties of some most common conducting polymers.

CP	Conductivity ($mScm^{-1}$)	Advantages
Polypyrrole (PPy)	10^3~5×10^4	High conductivity, High stability, Biocompatibility, High mechanical strength.
Polyaniline (PANI)	10^2~10^8	High conductivity, High stability, Water solubility.
Polythiophene (PTh)	10^{-1}~10^{-4}	Good optical property, Biocompatibility.
Poly(3,4-ethylenedioxythiophene) (PEDOT)	3×10^5~5×10^5	High conductivity, High stability, Water solubility, High mechanical strength, Biocompatibility.
Poly (paraphenylene vinylene) (PPV)	1~1×10^5	Good optical properties, High stability.

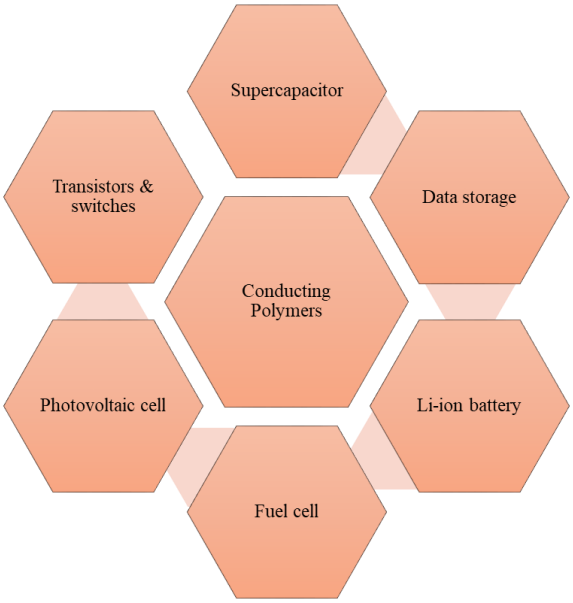

Figure 3. Applications of conducting polymers.

3. Famous Metal Oxides for Supercapacitor Application

MOs are a key factor in the development of sophisticated high-performance energy storage devices. Due to the high theoretical specific capacitance resulting from the faradaic charge transfer process, MOs have received significant attention for their use in supercapacitors; however, the low energy density of supercapacitors is a major drawback to their adoption. To address the issue of low energy density, MOs such as ruthenium oxide (RuO_2), manganese oxide (MnO_2), nickel oxide (NiO), cobalt oxide (Co_3O_4) and vanadium pentoxide (V_2O_5) have been widely explored as electrode materials. These MO materials have been identified as attractive candidates for electrodes in energy storage devices due to their wide surface area, possibility of synthesis in various component morphologies and multiple oxidation states (+1 to +7) [44]. Furthermore, they play a key role in the electrodes of electrochemical supercapacitors, and by modifying and managing their flaws and surface/interfaces on a nanoscale, they may significantly improve capacitance. Although their energy density has improved to some extent, their low electrical conductivity,

unpredictable volume expansion and slow ions transport in the bulk phase have limited their practical applications [45,46]. The most common MOs used in supercapacitors include RuO_2, MnO_2, NiO, Co_3O_4 and V_2O_5. Here, Figure 4 displays a graphical representation of various MOs with their theoretical specific capacitance values [44]. Briefly elaborated below are the most famous MOs used in supercapacitor application. The latest examples from the literature are included to justify their use.

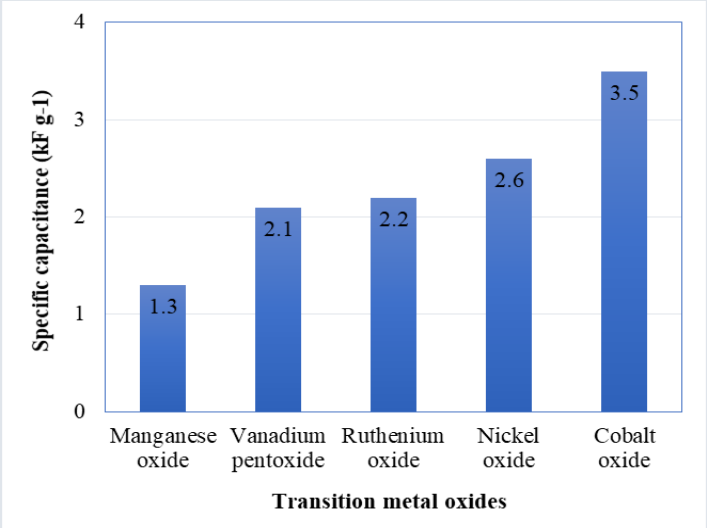

Figure 4. Comparison of the theoretical specific capacitances of different TMOs.

Ruthenium oxide (RuO_2)

RuO_2 is a dormant supercapacitor material owing to its outstanding capacitive performance. It has a higher rate capability, superior electrical conductivity, great cycling stability, superior charge-carrying properties, stability at low temperature and excellent conductivity. Although the high cost of ruthenium prevents the broad commercialization of RuO_2 as an electrode material in supercapacitors, research into RuO_2 has helped to better understand what makes an effective pseudocapacitive material in aqueous electrolytes. The critical property of RuO_2 is its readily reversible redox reactions and chemical stability compared to other MOs [47,48]. This is one of the main reasons for its high specific capacitance values. In the experiment performed by Ates and Yildirim, RuO_2/PANI and rGO/RuO_2/PANI nanocomposites were chemically synthesized, yielding specific capacitances 40.2 F g^{-1} and 723.09 F g^{-1}, respectively [48]. In the experiment carried out by Zhang et al., the optimized PANI/RuO_2 electrode was prepared, and the highest specific capacity of 816 F g^{-1} was reported [49]. An experiment performed by Cho et al. proposed that electrode RuO_2 nanoneedles on Ta/Cu foil exhibited a remarkable specific capacitance of 1420 F g^{-1} at a scan rate of 5 mV s^{-1} and excellent cycling stability, i.e., ~98% of capacitance retention at 100 mV s^{-1} after several hundred cycles. The electrode also showed a high energy density of ~13 Wh kg^{-1} at a power density of 27 kW kg^{-1} [50]. Deshmukh et al. prepared PANI–RuO_2 composite thin films, which demonstrated the maximum specific capacitance of 830 F g^{-1}. The films exhibited the specific energy and specific power densities of 216 W h kg^{-1} and 4.16 kW kg^{-1}, respectively [51]. The same composite was synthesized using a successive ionic layer adsorption and reaction (SILAR) method, which yields a specific capacitance of 664 F g^{-1} and higher capacitance retention (89%) of its initial capacitance after 5000 cycles [52]. In an experiment demonstrated by Thakur and Lokhande, RuO_2-incorporated PPy hybrid flexible electrodes were prepared, whose specific capacitance was found to be 1010.4 F g^{-1} at 5 mV s^{-1} in 0.2 M of Na_2SO_4 [53]. An experiment carried by Liu et al. reported that the synthesis of composite RuO_2/PEDOT nanotubes showed a high specific capacitance of 1217 F g^{-1}. The nanotubes exhibited a high power density of 20 kW kg^{-1} while maintaining 80% energy density (28 Wh kg^{-1}) of their maximum value [54].

Manganese oxide (MnO_2)

MnO_2 is another attractive MO which is widely employed in oxidation catalyst materials, aqueous batteries, supercapacitors and other industries due to its large reserves, low toxicity and simple fabrication procedure. It is regarded as one of the most promising electrode materials, particularly for supercapacitors. Due to its exceptional environmental friendliness and high theoretical specific capacity, MnO_2 is a great faradaic material that can be utilized as an alternate MO. It also has a higher operational capacity and is more cost effective. The reasons for the outstanding performance of MnO_2 can be divided into two categories. MnO_2 has outstanding electrochemical properties, including a high theoretical capacity (1370 F g^{-1}), which refers to the single-electron redox reaction of each Mn atom, a wide potential window (0.9–1.0 V); and excellent electrochemical properties in neutral electrolyte, which leads to low chemical corrosion of the collector [44,55,56]. Several crystallographic structures of MnO_2 are found, namely α-MnO_2, β-MnO_2, γ-MnO_2, δ-MnO_2 and λ-MnO_2, and the specific capacitance measured for MnO_2 mainly depends on the crystallographic structure, which decreases in the following order: α(m) > α > δ > γ > λ > β [57]. Mn ion is found in the five oxidation states: +2, +3, +4, +6 and +7, and oxidation state is a critical factor affecting the specific capacitance [58]. However, due to the weak conductivity of MnO_2, the actual specific capacitance is far less than the theoretical specific capacitance. Furthermore, MnO_2 has weak structural stability and is easily dissolved in the electrolyte, resulting in poor cycling ability. Moreover, it does not have a high electron-transporting capacity, which restricts the material's capacitive efficiency and prevents it from exhibiting high-power performance, limiting its use in energy storage devices [59]. Zhao and Wang fabricated nano-network MnO_2/PANI (MP) composites whose highest attainable specific capacitance could reach up to 497 F g^{-1}. It also exhibited good cycle stability with the cycle retention of 88.2% after 5000 cycles at 10 A g^{-1} [60]. Liu et al. synthesized ternary hierarchical nanofibers MnO_2/PANI/MWCNT. These exhibited the highest capacitance of 348.5 F g^{-1} at 1 A g^{-1} and maintained capacitance retention of 88.2% after 2000 consecutive cycles [61]. Grover et al. fabricated an asymmetric supercapacitor with coaxial MWCNT/PANI using MnO_2 as a positive electrode and MWCNT as a negative electrode, whose specific capacitance was found to be 324 F g^{-1} at a scan rate of 2 mA cm^{-2}. It showed 78% retention of capacitance after 3000 cycles at 3 mA cm^{-2} [62]. Pan et al. reported PANI@MnO_2/graphene composites. A specific capacitance of 695 F g^{-1} was obtained after 1000 cycles at a current density of 4 A g^{-1} [63]. Li et al. fabricated carbon cloth /MnO_2/PANI nanofibers, which delivered specific capacitance up to 728.7 F g^{-1} at 1 A g^{-1}. They exhibited capacitance retention of 87% after 2000 cycles [64]. Yin et al. fabricated PEDOT:PSS/MnO_2 hybrids, which revealed a remarkable specific capacitance of 365.5 F g^{-1} at a current density of 1 A g^{-1}. The hybrids exhibited retention after 2000 cycles [65].

Nickel oxide (NiO)

When compared to other MOs (such as RuO_2), NiO is a better supercapacitor electrode because it has a higher theoretical capacitance of 2584 F g^{-1}. It is also employed in supercapacitors because of its high surface area and non-toxicity. The cheap production cost and low environmental impact make NiO a viable substitute. Due to Ni's numerous oxidation states, oxides of Ni are particularly fascinating. Nonetheless, in experiments, Ni's lower electrical conductivity and smaller accessible surface areas result in poor reversibility and limited capacitance during the charge and discharge process. A better answer to this conundrum is to increase the active surface area of objects by converting them from bulk systems to porous/hollow designs [44,66,67]. Singu et al. prepared PANI-NiO nanocomposites. These showed high specific capacitances up to 514 Fg^{-1} at a scan rate of 1 mV s^{-1} [68]. Zhang et al. fabricated ACNF/PANI/NiO ternary composites as electrode materials for supercapacitors, which exhibited an outstanding specific capacitance of 1157 Fg^{-1} and displayed a remarkable capacitance retention of 93.89% after 5000 cycles [69]. Cho et al. fabricated NiO/PANI: PSS nanocomposites, which displayed higher capacitance (834 F g^{-1}) at 1 A g^{-1}. These showed an outstanding cycling life, i.e., 88.9% retention of specific

capacitance after 3000 charge/discharge cycles with an energy density of 32.84 Wh kg^{-1} and a power density of 375 W kg^{-1} [70]. Yang et al. prepared a hybrid electrode comprising NiO/Ni $(OH)_2$/PEDOT, which delivered a high specific capacitance of 404.1 mF cm^{-2} at a current density of 4 mA cm^{-2} and a long cycle life with 82.2% capacitance retention after 1000 cycles. It revealed an energy density of 0.011 mWh cm^{-2} at a power density of 0.33 mW cm^{-2} at a voltage window of 1.45 V [71]. Han et al. reported NiO/PPy-6, which showed a high specific capacitance of 3648.6 F g^{-1} at 3 A g^{-1} and remarkable rate capability, i.e., 1783 F g^{-1}, at a high current density of 30 A g^{-1}. An asymmetric supercapacitor (ASC) was fabricated using NiO/PPy-6 and AC as the positive electrode and the negative electrode, respectively. NiO/PPy-6//AC achieved a high specific capacitance of 937.5 F g^{-1} at 3 A g^{-1} and a high energy density of 333.3 W h kg^{-1} at a power density of 2399.99 W kg^{-1} [72].

Cobalt oxide (Co_3O_4)

Due to its strong redox characteristics, theoretical high capacitance and simple synthesis, Co_3O_4 is emerging as the best feasible supercapacitor material. It is the ideal substitute for using high-cost, non-environmentally friendly RuO_2, because Co_3O_4 has two electronic states, Co^{3+} and Co^{2+}. Different methodologies have been developed to generate different types of cobalt oxide-based nanocomposites with higher charge storage capability. An outstanding electrochemical capacitive behaviour is revealed by Co_3O_4 electrode material with special microstructures and morphology. However, in practice, the capacitance differs significantly from the theoretical value. Due to low conductivity, sluggish kinetics, huge volume expansion-contraction and severe particle aggregation, electron transport is hampered. As a result, the capacitance and cycling performance of Co_3O_4 are limited. Despite this, the limited electric conductivity makes cycling stability and rate capabilities difficult. As a result, significant efforts have been made in the development of nanostructured Co_3O_4 to improve electrochemical performance. Co_3O_4 electrode material has poor conductivity. The creation of a Co_3O_4 composite will result in a high ranking performance, eliminating the drawback of using a single electrode material [44,45,73,74]. Ren et al. prepared hierarchically hollow Co_3O_4/polyaniline nanocages (Co_3O_4/PANI NCs) that revealed a large specific capacitance of 1301 F g^{-1} at the current density of 1 A g^{-1}, energy density of 41.5 Whkg^{-1} at 0.8 kW kg^{-1}, and outstanding power density of 15.9 kW kg^{-1} at 18.4 Wh kg^{-1}. The nanocages displayed superior cycling stability with 90 % capacitance retention after 2000 cycles [75]. Zhenyin Hai et al. synthesized the core–shell PANI-Co_3O_4 nanocomposites whose specific capacitance was 1184 F g^{-1} at 1.25 A g^{-1}, and capacitance retention of 84.9% was achieved after 1000 charge/discharge cycles [76]. Lin et al. reported porous graphene/PANI/ Co_3O_4 (GPC) ternary hybrid aerogels with a high specific capacitance of 1247 F g^{-1} at a current density of 1 A g^{-1}, and no capacitance loss was observed for 3500 cycles [77]. Guo et al. fabricated hierarchical Co_3O_4@PPy core–shell composite nanowires (NWs) that exhibited a high specific capacitance of 2122 F g^{-1} at 5 mA cm^{-2} with a cycling stability of 77.8% capacitance retention over 5000 cycles at 25 mA cm^{-2} [78]. A PEDOT/GO/Co_3O_4 nanocomposite was prepared by Sulaiman et al. that exhibited a specific capacitance of 535.60 F g^{-1} and excellent cycle stability with the capacitance retention of 92.69% after 2000 cycles [79]. Yang et al. synthesized a Co_3O_4/PEDOT supercapacitor whose highest areal capacitance of 160 mF cm^{-2} at a current density of 0.2 mA cm^{-2} was reported; it achieved a high cycling stability of 93% capacitance retention after the 20,000th cycle [80].

Vanadium pentoxide (V_2O_5)

Due to its multiple oxidation states V^{2+} to V^{5+}, V_2O_5 is considered a promising super capacitive electrode among redox-active MOs. It features a distinctive layered structure, as well as a large potential window. Vanadium-based oxides are advantageous because of their high power density, natural abundance, low cost and theoretical specific capacity. Despite this, their application fields are limited because of structural instability and low electric conductivity. Vanadium dioxide (VO_2), vanadium trioxide (V_2O_3) and V_2O_5 are the most common vanadium oxides, with a valence of +5 being the most stable and +4 being

the least stable. Vanadium oxide has been extensively studied as an aqueous asymmetric supercapacitor device (AASCD) cathode electrode material [45,81]. Bai et al. prepared V_2O_5-PANI composite NWs that revealed a maximum specific capacitance of 443 F g^{-1} at 1.6 V potential window. They showed a maximum energy density of 69.2 Wh kg^{-1} at a power density of 720 W kg^{-1}, and a maximum power density of 7200 W kg^{-1} at an energy density of 33.0 Wh kg^{-1}. They also showed excellent stability, with 92% capacitance retention after 5000 cycles [82]. Asen et al. reported a V_2O_5/PPy/GO nanocomposite that yielded a specific capacitance of 750 F g^{-1} at a current density of 5 A g^{-1}, a maximum energy density of 27.6 Wh kg^{-1} at a power density of 3600 W kg^{-1}, and a maximum power density of 13,680 W kg^{-1} at an energy density of 22.8 Wh kg^{-1}. V_2O_5/PPy/GO maintained a cyclic stability of 83% capacitance retention after 3000 cycles [83]. Bi et al. prepared G-V_2O_5/PEDOT nanocable-based supercapacitors that showed an excellent specific capacitance of 614 F g^{-1} and an energy density of 85 Wh kg^{-1} in neutral aqueous electrolyte. A long cycling life with 122% capacitance retention after 50,000 cycles was achieved for these supercapacitors [84].

Ferrous oxide (Fe_3O_4)

Iron oxide is known to be one of the promising electrode materials due to its wide operating potential, high redox activity, low cost, abundant availability and eco-friendliness. The presence of iron oxide in various crystallographic forms such as, FeO (Wurtzite), α-Fe_2O_3 (Hematite), γ-Fe_2O_3 (Maghemite) and Fe_3O_4 (Magnetite) is based on the atomic arrangements of Fe^{3+} and O^{2-} ions. Among various crystallographic forms, hematite (α-Fe_2O_3) is one of the most stable, with a hexagonal corundum-like structure. Generally, the pseudocapacitive performance of Fe_2O_3 emerges from the reversible oxidation/reduction between Fe^{3+} and Fe^{2+}. High hydrogen evolution potential in the aqueous solution of iron oxide (Fe_xO_y) materials makes them favourable candidates for the negative electrode in SCs. Retardation of the charge storage capability and poor electronic conductivity (being—10–14 S cm^{-1}) results in their actual specific capacitance (120–300 F g^{-1}), which is far from the theoretical value [45,85,86]. In an experiment demonstrated by Prasanna et al., prepared polyaniline/ferric oxide nanocomposites revealed a maximum specific capacitance of 974 Fg^{-1} at a scan rate of 2 mVs^{-1} using cyclic voltammetry (CV), and C_{sp} equal to 857 F g^{-1} at a current density of 0.2 A g^{-1}. Further, the material also revealed a high energy density of 118 Wh kg^{-1} with a maximum power density of 9.8 kW kg^{-1}, and cyclic stability with capacitance retention of about 94% after 2000 cycles [87]. In an experiment, Yang et al. synthesized Fe_2O_3/PANI hybrid nanostructured hydrogels that exhibited a high specific capacitance of 473.6 F g^{-1} (236.8 mF cm^{-2}) at a current density of 1 A g^{-1} and good cycling stability, i.e., capacitance retention of 98.2% after 5000 cycles. Hybrid supercapacitors consisting of α-Fe_2O_3/PANI and PANI electrodes achieved a high energy density of 0.31 mWh cm^{-3} at a power density of 67.1 mW cm^{-3} [88].

Tungsten trioxide (WO_3)

WO_3 is an electrochemically stable n-type semiconductor MO that has a wide range of applications. Many investigations released in recent years have confirmed the viability of WO_3 as an energy storage material. Its electrochemical performance is aided by its high conductivity, attractive crystal structure and small radius. Due to various morphologies, its natural availability, low cost, high theoretical specific capacitance, higher electrochemical stability and environmental friendliness, WO_3 is considered a good contender for supercapacitors. The hexagonal phase (h-WO_3) is the most favourable for supercapacitor applications from several crystal forms of WO_3 [89–92]. Das et al. prepared a WO_3@PPy composite that showed excellent electrochemical properties with a higher specific capacitance of 586 F g^{-1} at 2 A g^{-1} than those of its individual components (WO_3: 402 F g^{-1} and PPy: 224 F g^{-1}) [93]. Zhuzheskii et al. reported a PEDOT/WO_3 composite film that exhibited a high specific capacitance of 689 Fg^{-1} in the potential window −0.3 to 0 V [94]. Samu et al. synthesized WO_3/PANI hybrid nanostructures and reported a specific capacitance of 350 F g^{-1} [95].

Tin oxide (SnO_2)

The n-type semiconducting material SnO_2 enables the fabrication of electrodes that could be used for supercapacitor applications due to its outstanding chemical properties. The nanostructured SnO_2 is the most advantageous MO due to its broad band gap of 3.6 eV, increased capacitance, low cost and lack of toxicity. SnO_2 has the advantage of being inexpensive and environmentally friendly [96,97]. Hu et al. prepared PANI/SnO_2 composites that show a specific capacitance up to 305.3 F g^{-1} with a specific energy density of 42.4 Wh kg^{-1} and 96% coulombic efficiency [98]. Wang et al. fabricated a nanocomposite of SnO_2@PANI (SP-2) with a high specific capacitance of 335.5 F g^{-1} at 0.1 A g^{-1}, a good rate capability of 108.8 F g^{-1} at 40 A g^{-1} and excellent cycling stability, i.e., no capacitance loss after 10,000 cycles [99].

4. CP-MO Composites for Supercapacitor Application

Each material has its own strengths and weaknesses, as do CPs and MOs. The CP-like PANIs have high conductivity, easy synthesis methods and a low cost, but their mechanical stability and tendency of degradation during repeated charge discharge cycles limits their application in supercapacitors. This is due to the swelling and shrinkage of CP because of associated ion and solvent transfer across the CP chains/electrolyte interface. PPy has good electrical conductivity and good environmental stability, but its non-porous structure does not allow the access of electrolytes during the redox cycling, which affects its cycling stability. PEDOT's porous structure provides electrolytic access, but it has a lower mass specific capacitance as compared to PANI and PPy. On the other hand, MOs have a high specific capacitance, are low in cost and have an abundant but relatively small surface area. Their low electrical conductivity and inability to withstand acidic solutions creates difficulties in the process of making electrodes for the supercapacitor. Combining both CP and MO by incorporating their advantages to develop and optimize a material at the nanoscale tends to create interesting nanocomposites. Nanocomposites are materials with a nanoscale structure that improves the macroscopic properties of a product. Nanocomposite materials have unique mechanical properties, barrier qualities, weight reduction, and better long-term heat, wear and scratch resistance. The nanocomposites of CPs are different due to increases in electrical breakdown strength, melting temperature, colour, magnetism and charge capacity, as well as expansion in the interaction zone. The features of nanocomposite electrodes are influenced by the morphology and the interfacial properties of the mixture, in addition to the individual materials utilised. The CP-MO nanocomposites offer advantages including the flexibility, toughness and coatability of polymers, as well as the hardness and durability of MOs. Additionally, they have some synergetic qualities that are distinct from those of the component materials. It has been demonstrated that utilising nanocomposite electroactive materials can significantly improve the properties of supercapacitors, such as specific surface area, electrical and ionic conductivities, specific capacitance, cyclic stability, and energy and power density [19,43,100–104]. Hence, CP-MOs nanocomposites have gained an important place in the list of materials used for supercapacitor application. In the work carried out by Shahabuddin et al., CP was doped with MO and a nanocomposite was synthesized. The synthesized material was tested for the application of a supercapacitor, as well as for photocatalysis. The results suggested that the nanocomposite showed better results than that shown by bare CP [105]. In an experiment performed by Raza et al., MO and CPs worked together as composites to overcome each other's limitations and create a possible composite material for supercapacitor applications [106]. Figure 5 shows that carbonaceous materials have a specific capacitance of up to 300 F g^{-1}, while CP and MOs have a high specific capacitance of up to 1000 F g^{-1} and 1300 F g^{-1}, respectively. However, the highest specific capacitance is shown by CP-MO composite materials such as CP/MnO_2, CP/RuO_2 and CP/Co_3O_4, and CP carbonaceous material composites such as GO/CP, CNT/CP, AC/CP, etc., which show specific capacitance up to 2300 F g^{-1} [7].

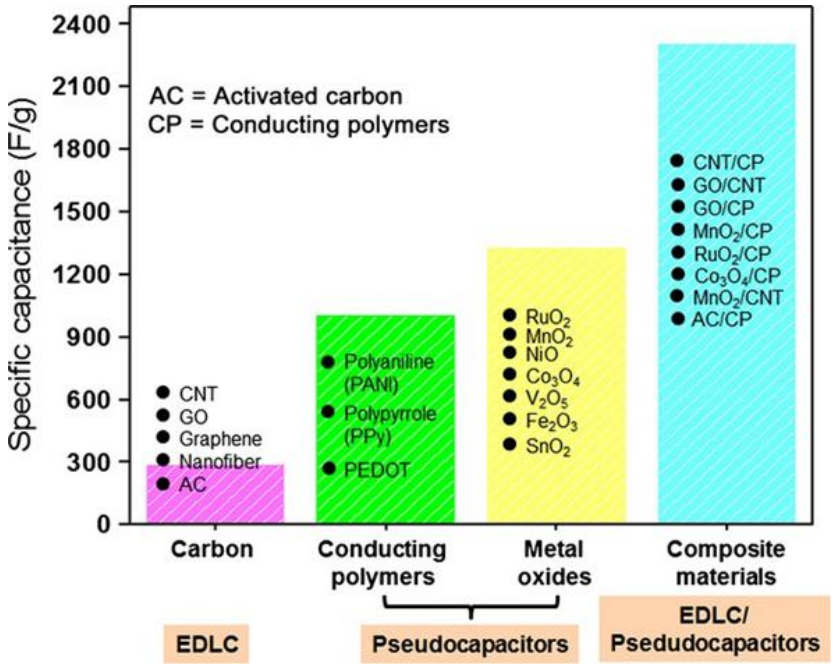

Figure 5. Comparison of various materials according to their specific parameter for supercapacitor application. Reproduced with permission from [7] (Shown et al.).

Table 2 summarizes the very recent data on numerous CP-MO nanocomposites with additional materials, their specific capacitance, energy densities, power densities, cycling stability and electrolytes. The table illustrates that the highest specific capacitance reported in a PANI/Co_3O_4//AC ternary nanocomposite is 3105.46 F g^{-1}, which possess good cycling stability up to 3000 cycles with 74.81% capacitance retention. The same nanocomposite exhibits the highest energy density of 250 Wh kg^{-1}; however, the NiO/Ni@C/PEDOT/AC nanocomposite exhibits the highest power density. The most adaptable conducting polymer is PANI, which may be used to create nanocomposites with metal and lanthanide oxides such as cerium oxide and samarium oxide. PANI-rGO-ZnO exhibits the lowest specific capacitance at roughly 40 F g^{-1}. Even though it has low specific capacitance, the cycling stability of the composite is good, i.e., the material shows 86% capacitance retention for 5000 cycles, while ternary nanocomposite PANI/Co_3O_4//AC displays the highest specific capacitance of 3105.46 F g^{-1}. Furthermore, cobalt oxide PANI ternary composites exhibit specific capacitance >1000 Fg^{-1}. PANI/Co_3O_4 has the highest energy density of 250 Wh kg^{-1} ternary nanocomposite. Moreover, MnO_2/PANI nanocomposites with carbon fibre and AC show the greatest capacitance. PANI/Fe_2O_3 nanocomposite and PANI/HY/SnO_2 also demonstrate high specific capacitances, i.e., 1669.18 and 1085 F g^{-1}, respectively, and it is reported that PANI/Fe_2O_3 is stable up to 25,000 cycles with capacitance retention of 96.5%. Co_3O_4 anchored PANI binary composite with a power density of 6.4 kW/kg has the highest power density among polyaniline nanocomposites. Additionally, there are several nanocomposites with MOs with PPy. The maximum specific capacitance of 1296 F g^{-1} and the highest power density of 5310.26 W kg^{-1} with 90% capacitance retention after 11,000 cycles were achieved by SnO_2QDS/PPy/GO nanocomposite. NiO-CoO-Ppy nanosheets also showed specific capacitance >1000 F g^{-1}, while Ni foam-MnO_2//Ni-foam PPY exhibited the lowest specific capacitance, measuring 59.29 mF cm^{-2}. Compared to PANI and PPy, PEDOT exhibited fewer nanocomposites with TMOs. pfCNFs/PEDOT/Co_3O_4//NDG nanocomposite exhibited the highest specific capacitance of 849.65 F g^{-1}, whereas NiO/Ni@C//PEDOT-AC nanocomposite exhibited the highest power density of 12,920 W kg^{-1}. V_2O_5@PEDOT nanobelts/graphene had the lowest specific capacitance, i.e., 22.4 mF cm^{-2}, and 92.4% capacitance retention after 50,000 cycles. Most of the experiments were carried out by using Na_2SO_4, H_2SO_4 and KOH as electrolytes.

Table 2. Latest reports on CP-MO based nanocomposites for supercapacitor application.

Conducting Polymer	Metal Oxide	Additional Material	Specific Capacitance (F/g)	Energy Density (Wh/kg)	Power Density (W/kg)	Cycling Stability (Cycles, % Capacitance Retention)	Electrolyte	Ref.
PANI	MnO_2	-	417	11.4	875	2000, 96.4%	1 M H_2SO_4	[107]
PANI	MnO_2	CC	1105 mF cm^{-2}	10.4 mW cm^{-3}	1.5 mWh cm^{-3}	2000, 86.35%	0.5 M H_2SO_4	[108]
PANI	MnO_2	$Ti_3C_2T_x$ MXene	21.1	47.25 µWh cm^{-2}	2.40 mW cm^{-2}	4000, 83%	PVA/ H_2SO_4	[109]
PANI	γ MnO_2	CF	654.3	30.9	750	5000, 73.2%	0.2 M H_2SO_4	[110]
PANI	MnO_2	MoS_2	259	35.97	500	4000, 94.1% at 16 A g^{-1}	1 M H_2SO_4	[111]
PANI	γ-MnO_2	_	642.5	114.2	798.6	-		[112]
PANI	Ag@MnO_2	AC	1028.66	49.77	1599.75	5000, 88.4%	2 M KOH	[113]
PANI	MnO_2	Hollow mesoporous silica	428.6	88.4	800	5000, 97.7%	6.0 M KOH	[114]
PANI	MnO_2	Porous carbon nanofiber (PCNF)	289	119	322	5000, 86%	1 M H_2SO_4	[115]
PANI	Mn_3O_4	graphene	460	23	600	4000, 89%	1 M H_2SO_4	[116]
PANI	NiO	-	480	-	-	-	-	[117]
PANI	NiO	Sulfonated graphene (SGO)	308.8	109.8	800	5000, 92.23%	6 M KOH	[118]
PANI	RuO_2	Ta_2O_5	428	26.7	2400	-	0.5 M H_2SO_4	[119]
PANI	RuO_2	rGO	723.09	-	-	-	1 M H_2SO_4	[48]
PANI	RuO_2, TiO_2	-	67.4	3.37	60	10,000, 81.6%	0.1 M H_2SO_4	[120]
PANI	Co_3O_4	-	1308	250	6400	-	1 M H_2SO_4	[121]
PANI	Co_3O_4	AC	3105.46	58.84	160	3000, 74.81%	6 M KOH	[122]
PANI	Co_3O_4 (FNCO, Fe-Ni co-doped)	-	1171	144	-	2000, 84%	1 M H_2SO_4	[123]
PANI	Co_3O_4	ZIF-8NPC	1407	52.81	751.51	-	KOH	[124]
PANI NP	Fe_2O_3	-	1669.18	-	-	25,000, 96.5%	KOH	[125]

Table 2. *Cont.*

Conducting Polymer	Metal Oxide	Additional Material	Specific Capacitance (F/g)	Energy Density (Wh/kg)	Power Density (W/kg)	Cycling Stability (Cycles, % Capacitance Retention)	Electrolyte	Ref.
PANI	Fe_2O_3	rGO	610.4	-	-	-	-	[126]
PANI	SnO_2	HY zeolite (solid acid) doped	1085	-	-	-	-	[127]
PANI	SnO_2	-	337	-	-	-	1 M H_2SO_4	[128]
PANI	SnO_2	TiO_2	540	27	200	6000, 85%	1 M H_2SO_4	[129]
PANI	h-WO_3	-	636	29.0	610	2000, 89% at 2 A g^{-1}	1 M H_2SO_4	[130]
PANI	WO_3	-	180	12.25	1075.6	10,000, 70%	-	[131]
PANI	ZnO Y_2O_3	-	873	73	9100	-	-	[132]
PANI	ZnO	rGO	~40	~5.61	~403	5000, 86%	1 M H_2SO_4	[133]
PANI	ZnO	ZIF-8-CC	4839–3987 mF cm^{-2}	0.137–0.0891 mW h cm^{-3}	1.421–23.629 W cm^{-3}	-	PVA/KCl gel	[134]
PANI	MoO_3	SiO_2, mesoporous carbon (MC)	45	31	155	250,000, 57%	1 M H_2SO_4	[135]
PANI	CeO_2	HCl	504	100.8	830	-	0.1 M Na_2SO_4	[136]
PANI	CeO_2	p-toluene sulfonic acid (PTSA)	454	100.8	830	-	0.1 M Na_2SO_4	[136]
PANI	CeO_2	rGO	684	46.27	850	6000, 92% at 4 A g^{-1}	1 M H_2SO_4	[137]
PANI	Sm_2O_3	TiO_2	881	141	-	1000, 91%	1 M H_2SO_4	[138]
PPy	MnO_2	Ni foam	59.29 mF/cm^2	42.99 to 77.94 μWh/cm^2	0.272 to 6.818 mW/cm^2	10,000, 95.6%	$LiClO_4$	[139]
PPY	MnO_2	CC	270	165.3	1000	1000, 94%	-	[140]
PPy	MnO_2	C_3N_4	509.4	63.9	2000	5000, 95.7%	1 M aqueous Na_2SO_4	[141]

Table 2. *Cont.*

Conducting Polymer	Metal Oxide	Additional Material	Specific Capacitance (F/g)	Energy Density (Wh/kg)	Power Density (W/kg)	Cycling Stability (Cycles, % Capacitance Retention)	Electrolyte	Ref.
PPy	MnO_2	Carbon nanofiber	-	0.340 mWh Cm^{-2}	1.5 $mWCm^2$	-	-	[142]
N-CNWs derived from PPy	$Ni@MnO_2$	CC	571.4	36.4	900	3500, 72.8%	4 mM $NaHCO_3$	[143]
PPy	MnO_2	CB	273.2	0.5513	91.556	1000, 92.20%	1 M H_2SO_4	[144]
PPy	MnO_2	$Ti_3C_2T_x$	61.5 mF cm^{-2}	6.73 µWh cm^{-2}	-	5000, 80.7%	(PVA/H_2SO_4) as the quasi-solid	[145]
PPy	Mno2	CNT	10.7	4.82	1382	5000, 86%	LiCl/PVA	[146]
PPy	NiO	-	679	94.4	500.74	1000, 83.9%	0.1 M $LiClO_4$	[147]
PPy	NiO	CoO	1123	35.9	801	5000, 90.1%	2 M KOH	[148]
PPy	NiO	Graphene	970.85	33.71	-	-	6 M KOH	[149]
PPy	TiO_2	rGO	462.1	-	-	-	2 M KOH	[150]
PPy	ZnO	-	161.02	-	-	5000, 70.71%	1 M KCl	[151]
PPy	FeO_x	-	2.0 F cm^{-2}	3.44 mWh cm^{-3}	6.72 mW cm^{-3}	10,000, 105.6%	3 M LiCl	[152]
PPy	Fe_2O_3	CC	237 mF cm^{-2}	24.2	408.2	10,000, 80% At 10 mA cm^{-2}	1 M Na_2SO_4	[153]
PPy	Fe_2O_3	rGO	626.8	87.05	500	-	1 M H_2SO_4	[154]
PPy	Fe_2O_3NTs	-	530 mF cm^{-2}	51.2	285.4	5000, 83.5%	1 M Na_2SO_4	[155]
PPy	SnO_2	CC	493.8 mF cm^{-2}	0.7 mWh cm^{-3}	4.74 mW cm^{-3}	10,000, 90.5%	PVA-KOH Gel	[156]
PPy	SnO_2 QDs	GO	1296	29.6	5310.26	11,000, 90%	(PVA/KOH) gel	[157]
PPy	V_2O_5	f-CNT	1266 mF cm^{-2}	-	-	-	1 M Na_2SO_4	[158]
PPy	MoO_3	rGO	412.3	19.8	301	6000, 85.1% at 2 A g^{-1}	Na_2SO_4	[159]

Table 2. *Cont.*

Conducting Polymer	Metal Oxide	Additional Material	Specific Capacitance (F/g)	Energy Density (Wh/kg)	Power Density (W/kg)	Cycling Stability (Cycles, % Capacitance Retention)	Electrolyte	Ref.
PPy	MoO_3	-	453.75	20.3	400	5000, 84.3%	1.0 M Na_2SO_4	[160]
PPy	Co_3O_4	N-doped MWCNT	~872	-	-	10,000, 96.8 %	KOH	[161]
PPY	Co_3O_4NW	MnO_2	215	41.3	4348	1000, 96.8%	-	[162]
PEDOT	MnO_2	V_2O_5	116.9 mF cm^{-2}	15.1 μWh cm^{-2}	-	10,000, 87.2%	Carboxymethyl cellulose sodium (CMC)-Na_2SO_4 gel	[163]
PEDOT	MnO_2	HNO_3 pre-treated biochar	76.6	14.0	53.1	-	-	[164]
PEDOT:PSS	MnO_2	CNT	105.2 mF·cm^{-2}	13.2 μW h·cm^{-2}	162 μW·cm^{-2}	-	1 M Na_2SO_4	[165]
PEDOT	MnO_2	Nanocrystalline cellulose (NCC)	144.69	10.3	494.9	2000, 83%	1 M KCl	[166]
PEDOT: PSS	MnO_2	-	550	18	4500	-	-	[167]
PEDOT	NiO/Ni@C	AC	805.3	20.7	12,920	10,000, 69.7%	6 M KOH	[168]
PEDOT	Ni^{2+}/NiO-SS	-	236	40.15 Ah/Kg	1320	2500, 99%	0.1 M $TBAPF_6$/PC	[169]
PEDOT	V_2O_5	Graphene	22.4 mF cm^{-2}	0.18 μW h cm^{-2}	11 μW cm^{-2}	50,000, 92.4%	5 M LiCl	[170]
PEDOT	Co_3O_4	Carbon nanofibers	849.65	14.54	1726.96	-	-	[171]
PEDOT: PSS	WO_3	-	701 mF cm^{-2}	0.083 mWh cm^{-2}	10 mW $cm^{-2.}$	10,000, 96%	0.1 M H_2SO_4	[172]
PEDOT	CeO_2	C	141.56	11.12	2000	-	1 M Na_2SO_4	[173]
PEDOT: PSS	MoO_3	-	15.7 mF cm^{-2}	0.623 μW h cm^{-2}	40 μW cm^{-2}	11,000, 92.4%	2 M Na_2SO_4	[174]
PTh	TiO_2	PANI	265	9.09	3770	3000, 92.3%	1 M H_2SO_4	[175]

5. Conclusions

This report offered an outlook on CP/MO with their examples and application in supercapacitors. The discussion began with the introduction of supercapacitors, their types, and the need for developing energy storage devices. Supercapacitors or ultracapacitors have been acknowledged as appropriate energy storage devices to meet future demands for a number of applications, such as electronic gadgets and hybrid electric vehicles, to fulfil the demand for sustainable and renewable energy storage. Developments in MO, CP and their advantages in CP/MO-based nanocomposites have been highlighted and summarized. We recently revealed the importance of preparing superior quality CP/MO nanocomposites made by CP grafting on various nanomaterials/MOs. This approach helps to overcome the drawbacks of CP/MO nanocomposites obtained by merely mixing these two components. The field of nanocomposites has been challenging but it continues to grow. Although CP/MO nanocomposites can provide good electrochemical performance, these individual pseudocapacitor materials have some limitations, such as low conductivity of metal oxide and less cycling stability of conducting polymers. Even if the ideal synthesis of CP/MO-based nanocomposites is believed to overcome the disadvantages of each component, scalable and flexible energy storage devices require further improvements in the supercapacitive performances of the materials, such as specific capacitance, specific energy, long-term stability, etc. Finding suitable CP/MO ratios as active material and developing justifiable charge storage mechanisms by studying underlying reactions is always challenging in electrode materials that include a binary, ternary or even quaternary mixture of various materials. To summarise, significant efforts should be made to advance CP/MO-based materials to broaden the scope of supercapacitors to be included in flexible and compressible devices.

Author Contributions: P.H.P. and V.V.K.: writing—original draft preparation, writing—review and editing; S.A.J.: writing—review and editing, supervision and project administration. All authors have read and agreed to the published version of the manuscript.

Funding: This research received no external funding.

Data Availability Statement: Not applicable.

Conflicts of Interest: The authors declare no conflict of interest.

Abbreviations

AASCD	Aqueous asymmetric supercapacitor device
AC	Activated carbon
ACNF	Activated carbon nanofibers
ASC	Asymmetric supercapacitor
C	Carbon
CB	Carbon black
CC	Carbon cloth
CDC	Carbide-derived carbon
CF	Carbon fibre
CMC	Carboxymethyl cellulose
CNT	Carbon nanotubes
CP	Conducting polymer
CV	Cyclic voltammetry
EDLC	Electrical double-layer capacitor
F-CNT	Functionalized carbon nanotube
FNCO	Fe-Ni co-doped
GO	Graphene oxide
GPC	Graphene/polyaniline/Co_3O_4
LED	Light-emitting diode
MC	Mesoporous carbon
MO	Metal oxides

MPHMS	MnO_2/polyaniline/hollow mesoporous silica
MWCNT	Multiwalled carbon nanotubes
NC's	Nanocages
NCC	Nanocrystalline cellulose
N-CNWs	Nitrogen-doped carbon nanowires
NPC	Nanoporous carbon
NW's	Nanowires
PA	Polyacetylene
PANI	Polyaniline
PCNF	Porous carbon nanofiber
PEDOT	Poly (3,4 ethylene dioxy thiophene)
PLED	Polymer light-emitting diode
PPP	Polyparaphenylene
PPS	Polyparaphenylene sulphide
PPV	Polyparaphenylene vinylene
PPy	Polypyrrole
PSS	Polystyrene sulphonate
PTh	Polythiophene
PTSA	p-toluene sulphonic acid
PVA	Polyvinyl alcohol
QD	Quantum dot
rGO	Reduced graphene oxide
SC	Supercapacitors
SGO	Sulphonated graphene oxide
SILAR	Successive ionic layer adsorption and reaction
$TBAPF_6$/PC	Tetra-n butylammonium hexafluorophosphate/propylene carbonate
ZIF-8-CC	Zeolitic imidazolate framework-carbon cloth

References

1. Kondawar, S.B. Supercapacitors. In *Conducting Polymer Nanocomposites for Supercapacitors*; Smithers Rapra Technology Ltd.: Shrewsbury, UK, 2015; pp. 1–24.
2. Lonkar, S.P.; Pillai, V.V.; Patole, S.P.; Alhassan, S.M. Scalable In Situ Synthesis of 2D–2D-Type Graphene-Wrapped SnS_2 Nanohybrids for Enhanced Supercapacitor and Electrocatalytic Applications. *ACS Appl. Energy Mater.* **2020**, *3*, 4995. [CrossRef]
3. Huang, S.; Zhu, X.; Sarkar, S.; Zhao, Y. Challenges and Opportunities for Supercapacitors. *APL Mater.* **2019**, *7*, 100901. [CrossRef]
4. Pan, H.; Li, J.; Feng, Y.P. Carbon Nanotubes for Supercapacitor. *Nanoscale Res. Lett.* **2010**, *5*, 654. [CrossRef] [PubMed]
5. Majumdar, D.; Mandal, M.; Bhattacharya, S.K. Journey from supercapacitors to supercapatteries: Recent advancements in electrochemical energy storage systems. *Emergent Mater.* **2020**, *3*, 347. [CrossRef]
6. Xie, A.; Tao, F.; Jiang, C.; Sun, W.; Li, Y.; Hu, L.; Du, X.; Luo, S.; Yao, C. A Coralliform-Structured γ-MnO_2 /Polyaniline Nanocomposite for High-Performance Supercapacitors. *J. Electroanal. Chem.* **2017**, *789*, 29. [CrossRef]
7. Shown, I.; Ganguly, A.; Chen, L.; Chen, K. Conducting Polymer-based Flexible Supercapacitor. *Energy Sci. Eng.* **2015**, *3*, 2–26. [CrossRef]
8. Bolgam, R.; Boddula, R.; Srinivasan, P. Improving electrochemical performance by sulphonation of polyaniline-graphene-silica composite for high performance supercapacitor. *Int. J. Polym. Mater. Polym. Biomater.* **2016**, *65*, 835. [CrossRef]
9. Huo, S.; Zhao, Y.; Zong, M.; Liang, B.; Zhang, X.; Khan, I.U.; Song, X.; Li, K. Boosting supercapacitor and capacitive deionization performance of hierarchically porous carbon by polar surface and structural engineering. *J. Mater. Chem. A* **2020**, *8*, 2050. [CrossRef]
10. Bolgam, R.; Boddula, R.; Srinivasan, P. Synthesis of highly crystalline polyaniline with the use of (cyclohexylamino)-1-propanesulphonic acid for supercapacitor. *J. Appl. Electrochem.* **2015**, *45*, 51. [CrossRef]
11. Boddula, R.; Srinivasan, P. Simultaneous Oxidation and Doping of Aniline to Polyaniline by Oxidative Template: Electochemical Performance in Supercapacitor. *Int. J. Polym. Mater. Polym. Biomater.* **2015**, *64*, 939. [CrossRef]
12. Yumak, T.; Bragg, D.; Sabolsky, E.M. Effect of Synthesis Methods on the Surface and Electrochemical Characteristics of Metal Oxide/Activated Carbon Composites for Supercapacitor Applications. *Appl. Surf. Sci.* **2019**, *469*, 983. [CrossRef]
13. Nandhini, S.; Rajagopalan, T.; Muralidharan, G. Copper Incorporated Nickel Sulphide on Ni-Foam: Binder-Free Electrode for High Performance Supercapacitors. *AIP Conf. Proc.* **2020**, *2265*, 030597. [CrossRef]
14. Li, Y.; Zhou, M.; Xia, Z.; Gong, Q.; Lu, X.; Yang, Y.; Gao, Q. Facile Preparation of Polyaniline Covalently Grafted to Isocyanate Functionalized Reduced Graphene Oxide Nanocomposite for High Performance Flexible Supercapacitors. *Colloids Surf. A* **2020**, *602*, 125172. [CrossRef]
15. Feng, Y.; Liu, W.; Wang, Y.; Gao, W.; Li, J.; Liu, K.; Wang, X.; Jiang, J. Oxygen Vacancies Enhance Supercapacitive Performance of $CuCo_2O_4$ in High-Energy-Density Asymmetric Supercapacitors. *J. Power Sources* **2020**, *458*, 228005. [CrossRef]

16. Vangari, M.; Pryor, T.; Jiang, L. Supercapacitors: Review of Materials and Fabrication Methods. *J. Energy Eng.* **2013**, *139*, 72. [CrossRef]
17. Yang, Y.; Chen, X.; Cao, Y.; Zhou, W.; Sun, H.; Chai, H. Facial Synthesis of Homogeneous Hollow Co_3O_4 Microspheres for Enhanced Cycle Life and Electrochemical Energy Storage Performance. *ChemElectroChem* **2020**, *7*, 723. [CrossRef]
18. Mulik, S.V.; Jadhav, S.A.; Patil, P.S.; Delekar, S.D. Transition metal oxide–conducting polymer nanocomposites and metal-organic framework-based composites for supercapacitor application. In *Advances in Metal Oxides and Their Composites for Emerging Applications*; Delekar, S.D., Ed.; Elsevier: Cambridge, MA, USA, 2022; pp. 135–186.
19. Awuzie, C.I. Conducting Polymers. *Mater. Today Proc.* **2017**, *4*, 5721. [CrossRef]
20. Sharma, S.; Sudhakara, P.; Omran, A.A.B.; Singh, J.; Ilyas, R.A. Recent Trends and developments in Conducting Polymer Nanocomposites for Multifunctional Applications. *Polymers* **2021**, *13*, 2898. [CrossRef]
21. Ragavan, K.V.; Neethirajan, S. Nanoparticles as Biosensors for Food Quality and Safety Assessment. In *Nanomaterials for Food Applications*; Elsevier Science: Amsterdam, The Netherlands, 2019; p. 147. [CrossRef]
22. Heeger, A.J.; MacDiarrmid, A.G.; Shirakawa, H. *The Nobel Prize in Chemistry, 2000: Conductive Polymers*; Royal Swedish Academy of Sciences: Stockholm, Sweden, 2000.
23. Mishra, A.K. Conducting Polymers: Concepts and Applications. *J. At. Mol. Condens. Matter Nano Phys.* **2018**, *5*, 159. [CrossRef]
24. Walton, D.J. Electrically conducting polymers. *Mater. Dec.* **1990**, *11*, 142. [CrossRef]
25. Namsheer, K.; Rout, C.S. Conducting Polymers: A Comprehensive Review on Recent Advances in Synthesis, Properties and Applications. *RSC Adv.* **2021**, *11*, 5659. [CrossRef]
26. Xia, C.; Chen, W.; Wang, X.; Hedhili, M.N.; Wei, N.; Alshareef, H.N. Highly Stable Supercapacitors with Conducting Polymer Core-Shell Electrodes for Energy Storage Applications. *Adv. Energy Mater.* **2015**, *5*, 1401805. [CrossRef]
27. Gupta, B.; Melvin, A.A.; Revathi, P.; Matthews, T.; Dash, S.; Tyagi, A.K.; Prakash, R. Conducting polymer-metal oxide nanocomposite and their property towards energy storage: An overview. In *Polymer-Matrix Composites Types, Application and Performance*; Kumar, R., Ed.; Nova Science Publishers, Inc.: New York, NY, USA, 2014; pp. 191–214.
28. Ravichandran, R.; Sundarrajan, S.; Venugopal, J.R.; Mukherjee, S.; Ramakrishna, S. Applications of conducting polymers and their issues in biomedical engineering. *JR Soc. Interface* **2010**, *7*, 559. [CrossRef] [PubMed]
29. Mahat, M.M.; Sabere, A.S.M.; Azizi, J.; Amdan, N.A.N. Potential Applications of Conducting Polymers to Reduce Secondary Bacterial Infections among Covid-19 Patients: A Review. *Emergent Mater.* **2021**, *4*, 279. [CrossRef] [PubMed]
30. Datta, M.; Maraz, K.M.; Rahman, N.; Khan, R.A. Applications of polymer in biomedical implication. *GSC Biol. Pharm. Sci.* **2021**, *14*, 98–114. [CrossRef]
31. Kausar, A. Emerging hybrid derived from polythiophene and graphene. In *Conducting Polymer Based Nanocomposites*; Elsevier: Cambridge, MA, USA, 2021; pp. 129–156.
32. Kumar, R.; Singh, S.; Yadav, B.C. Conducting Polymers: Synthesis, Properties and Applications. *Int. J. Adv. Res. Sci. Eng. Technol.* **2015**, *2*, 110. [CrossRef]
33. Bhandari, S. Polyaniline: Structure and Properties Relationship. In *Polyaniline Blends, Composites, and Nanocomposites*; Visakh, P.M., Pina, C.D., Falleta, E., Eds.; Elsevier: Cambridge, MA, USA, 2018; pp. 23–60.
34. Boddula, R.; Srinivasan, P. Role of dual dopants in highly ordered crystalline polyaniline nanospheres: Electrode materials in supercapacitors. *J. Appl. Polym. Sci.* **2015**, *132*, 42510. [CrossRef]
35. Bolgam, R.; Boddula, R.; Srinivasan, P. One-step preparation of sulphonated carbon and subsequent preparation of hybrid materials with polyaniline salt: A promising supercapacitor electrode material. *J. Solid State Electrochem.* **2017**, *21*, 1313. [CrossRef]
36. Srinivasan, P.; Boddula, R. Organic solvent soluble methyltriphynylphosphonium peroxodisulphate: A novel oxidant for synthesis of polyaniline in high performance supercapacitors. *New J. Chem.* **2015**, *39*, 5382. [CrossRef]
37. Deshmukh, K.; Basheer Ahamed, M.; Deshmukh, R.R.; Khadheer Pasha, S.K.; Bhagat, P.R.; Chidambaram, K. Biopolymer Composites with High Dielectric Performance: Interface Engineering. In *Biopolymer Composites in Electronics*; Sadasivuni, K.K., Ed.; Elsevier: Cambridge, MA, USA, 2017; pp. 27–128.
38. Mantione, D.; del Agua, I.; Sanchez-Sanchez, A.; Mecerreyes, D. Poly(3,4-Ethylenedioxythiophene) (PEDOT) Derivatives: Innovative Conductive Polymers for Bioelectronics. *Polymers* **2017**, *9*, 354. [CrossRef]
39. Lövenich, W. PEDOT-Properties and Applications. *Polym. Sci. Ser. C* **2014**, *56*, 135. [CrossRef]
40. Min, J.; Patel, M.; Koh, W.-G. Incorporation of Conductive Materials into Hydrogels for Tissue Engineering Applications. *Polymers* **2018**, *10*, 1078. [CrossRef] [PubMed]
41. Le, T.-H.; Kim, Y.; Yoon, H. Electrical and Electrochemical Properties of Conducting Polymers. *Polymers* **2017**, *9*, 150. [CrossRef]
42. Revin, S.B. Electrochemical Sensors for Biomolecules Using Functionalized Triazole Modified Conducting Polymer Electrodes. Ph.D. Thesis, Gandhigram Rural Institute, Chinnalapatti, India, 2012. [CrossRef]
43. Meng, Q.; Cai, K.; Chen, Y.; Chen, L. Research Progress on Conducting Polymer Based Supercapacitor Electrode Materials. *Nano Energy* **2017**, *36*, 268. [CrossRef]
44. Mohd Abdah, M.A.A.; Azman, N.H.N.; Kulandaivalu, S.; Sulaiman, Y. Review of the Use of Transition-Metal-Oxide and Conducting Polymer-Based Fibres for High-Performance Supercapacitors. *Mater. Dec.* **2020**, *186*, 108199. [CrossRef]
45. An, C.; Zhang, Y.; Guo, H.; Wang, Y. Metal Oxide-Based Supercapacitors: Progress and Prospectives. *Nanoscale Adv.* **2019**, *1*, 4644. [CrossRef]

46. Wu, Z.; Zhu, Y.; Ji, X.; Banks, C.E. Transition Metal Oxides as Supercapacitor Materials. In *Nanomaterials in Advanced Batteries and Supercapacitors*; Ozoemena, K.I., Chen, S., Eds.; Nanostructure Science and Technology; Springer International Publishing: Cham, Switzarland, 2016; pp. 317–344.
47. Zhang, Q.; Gu, D.; Li, H.; Xu, Z.; Sun, H.; Li, J.; Wang, L.; Shen, L. Energy Release from RuO_2//RuO_2 Supercapacitors under Dynamic Discharge Conditions. *Electrochim. Acta* **2021**, *367*, 137455. [CrossRef]
48. Ates, M.; Yildirim, M. The Synthesis of RGO/RuO_2, RGO/PANI, RuO_2/PANI and RGO/RuO_2/PANI Nanocomposites and Their Supercapacitors. *Polym. Bull.* **2020**, *77*, 2285. [CrossRef]
49. Zhang, G.; Deng, L.; Liu, J.; Wang, J.; Li, W.; Li, X. Controllable Intercalated Polyaniline Nanofibers Highly Enhancing the Utilization of Delaminated RuO_2 Nanosheets for High-Performance Hybrid Supercapacitors. *ChemElectroChem* **2022**, *9*, e202200039. [CrossRef]
50. Cho, S.; Kim, J.; Han, J.; Shin, G.; Park, S.; Yeon, S.; Jana, A.; Kim, H. Self-assembled RuO_2 nanoneedles on Ta/Cu foil for a robust and high-performance supercapacitor electrode. *Surf. Interfaces* **2022**, *31*, 102069. [CrossRef]
51. Deshmukh, P.R.; Bulakhe, R.N.; Pusawale, S.N.; Sartale, S.D.; Lokhande, C.D. Polyaniline–RuO_2 Composite for High Performance Supercapacitors: Chemical Synthesis and Properties. *RSC Adv.* **2015**, *5*, 28687. [CrossRef]
52. Deshmukh, P.R.; Patil, S.V.; Bulakhe, R.N.; Sartale, S.D.; Lokhande, C.D. Inexpensive Synthesis Route of Porous Polyaniline–Ruthenium Oxide Composite for Supercapacitor Application. *Chem. Eng. J.* **2014**, *257*, 82. [CrossRef]
53. Thakur, A.V.; Lokhande, B.J. Study of RuO_2 incorporated PPy hybrid flexible electrodes prepared by soaking and drying technique: A novel approach. *Appl. Phys. A* **2021**, *127*, 910. [CrossRef]
54. Liu, R.; Duay, J.; Lane, T.; Bok Lee, S. Synthesis and Characterization of RuO_2/Poly(3,4-Ethylenedioxythiophene) Composite Nanotubes for Supercapacitors. *Phys. Chem. Chem. Phys.* **2010**, *12*, 4309. [CrossRef] [PubMed]
55. Zhang, M.; Yang, D.; Li, J. Supercapacitor Performances of MnO_2 and MnO_2/ Reduced Graphene Oxide Prepared with Various Electrodeposition Time. *Vacuum* **2020**, *178*, 109455. [CrossRef]
56. Wu, D.; Xie, X.; Zhang, Y.; Zhang, D.; Du, W.; Zhang, X.; Wang, B. MnO_2/Carbon Composites for Supercapacitor: Synthesis and Electrochemical Performance. *Front. Mater.* **2020**, *7*, 2. [CrossRef]
57. Devaraj, S.; Munichandraiah, N. Effect of Crystallographic Structure of MnO_2 on Its Electrochemical Capacitance Properties. *J. Phys. Chem. C* **2008**, *112*, 4406. [CrossRef]
58. Wang, Z.; Yang, D.; Sham, T. Effect of Oxidation States of Manganese in Manganese Oxide Thin Films on their Capacitance Performances. *Surf. Sci.* **2018**, *676*, 71. [CrossRef]
59. Yu, J.; Li, M.; Wang, X.; Yang, Z. Promising High-Performance Supercapacitor Electrode Materials from MnO_2 Nanosheets@Bamboo Leaf Carbon. *ACS Omega* **2020**, *5*, 16299. [CrossRef]
60. Zhao, Y.; Wang, C.-A. Nano-Network MnO_2/Polyaniline Composites with Enhanced Electrochemical Properties for Supercapacitors. *Mater. Des.* **2016**, *97*, 512. [CrossRef]
61. Liu, W.; Wang, S.; Wu, Q.; Huan, L.; Zhang, X.; Yao, C.; Chen, M. Fabrication of Ternary Hierarchical Nanofibers MnO_2/PANI/CNT and Theirs Application in Electrochemical Supercapacitors. *Chem. Eng. Sci.* **2016**, *156*, 178. [CrossRef]
62. Grover, S.; Sahu, V.; Singh, G.; Sharma, R.K. High specific energy ternary nanocomposite polyaniline: Manganese dioxide@ MWCNT electrode for asymmetric supercapacitor. *J. Energy Storage* **2020**, *29*, 101411. [CrossRef]
63. Pan, C.; Gu, H.; Dong, L. Synthesis and Electrochemical Performance of Polyaniline @MnO_2/Graphene Ternary Composites for Electrochemical Supercapacitors. *J. Power Sources* **2016**, *303*, 175. [CrossRef]
64. Li, X.; Huang, H.; Zhang, P.; Zhai, X.; Chen, B.; He, Y.; Guo, Z. Rational preapaation of ternary carbon cloth/MnO_2/polyaniline nanofibers for high performance electrochemical supercapacitors. *J. Mater. Sci. Mater. Electron.* **2022**, *33*, 1918. [CrossRef]
65. Yin, C.; Zhou, H.; Li, J. Facile one-step hydrothermal synthesis of PEDOT: PSS/MnO_2 nanorod hybrids for high-rate supercapacitor electrode material. *Ionics* **2019**, *25*, 685. [CrossRef]
66. Vinodh, R.; Babu, R.S.; Atchudan, R.; Kim, H.-J.; Yi, M.; Samyn, L.M.; de Barros, A.L.F. Fabrication of High-Performance Asymmetric Supercapacitor Consists of Nickel Oxide and Activated Carbon (NiO//AC). *Catalysts* **2022**, *12*, 375. [CrossRef]
67. Sethi, M.; Shenoy, U.S.; Bhat, D.K. Hassle-Free Solvothermal Synthesis of NiO Nanoflakes for Supercapacitor Application. *Phys. B Condens. Matter* **2021**, *611*, 412959. [CrossRef]
68. Singu, B.S.; Palaniappan, S.; Yoon, K.R. Polyaniline–Nickel Oxide Nanocomposites for Supercapacitor. *J. Appl. Electrochim.* **2016**, *46*, 1039. [CrossRef]
69. Zhang, J.; Su, L.; Ma, L.; Zhao, D.; Qin, C.; Jin, Z.; Zhao, K. Preparation of Inflorescence-like ACNF/PANI/NiO Composite with Three-Dimension Nanostructure for High Performance Supercapacitors. *J. Electroanal. Chem.* **2017**, *790*, 40. [CrossRef]
70. Cho, E.C.; Chang-Jian, C.W.; Lee, K.C.; Huang, J.H.; Ho, B.C.; Ding, Y.R.; Hsiao, Y.S. Spray-dried nanoporous NiO/PANI: PSS composite microspheres for high performance asymmetric supercapacitors. *Compos. Part B* **2019**, *175*, 107066. [CrossRef]
71. Yang, H.; Xu, H.; Li, M.; Zhang, L.; Huang, Y.; Hu, X. Assembly of NiO/$Ni(OH)_2$ /PEDOT Nanocomposites on Contra Wires for Fiber-Shaped Flexible Asymmetric Supercapacitors. *ACS Appl. Mater. Interfaces* **2016**, *8*, 1774. [CrossRef] [PubMed]
72. Han, K.; Liu, Y.; Huang, H.; Goung, Q.; Zhang, Z.; Zhou, G. Tremella-like NiO Microspheres Embedded with Fish-Scale-like Polypyrrole for High-Performance Asymmetric Supercapacitor. *RSC Adv.* **2019**, *9*, 21608. [CrossRef] [PubMed]
73. Liang, R.; Du, Y.; Xiao, P.; Cheng, J.; Yuan, S.; Chen, Y.; Yuan, J.; Chen, J. Transition Metal Oxide Electrode Materials for Supercapacitors: A Review of Recent Developments. *Nanomaterials* **2021**, *11*, 1248. [CrossRef]

74. Wang, Z.; Wu, Z.; Meng, C.; Wu, L.; Yang, S.; Hong, X. Recent Advance in Co_3O_4 and Co_3O_4-Containing Electrode Materials for High-Performance Supercapacitors. *Molecules* **2020**, *25*, 269. [CrossRef] [PubMed]
75. Ren, X.; Fan, H.; Ma, J.; Wang, C.; Zhang, M.; Zhao, N. Hierarchical Co_3O_4/PANI Hollow Nanocages: Synthesis and Application for Electrode Materials of Supercapacitors. *Appl. Surf. Sci.* **2018**, *441*, 194. [CrossRef]
76. Hai, Z.; Gao, L.; Zhang, Q.; Xu, H.; Cui, D.; Zhang, Z.; Tsoukalas, D.; Tang, J.; Yan, S.; Xue, C. Facile Synthesis of Core–Shell Structured PANI-Co_3O_4 Nanocomposites with Superior Electrochemical Performance in Supercapacitors. *Appl. Surf. Sci.* **2016**, *361*, 57. [CrossRef]
77. Lin, H.; Huang, Q.; Wang, J.; Jiang, J.; Liu, F.; Chen, Y.; Wang, C.; Lu, D.; Han, S. Self-Assembled Graphene/Polyaniline/Co_3O_4 Ternary Hybrid Aerogels for Supercapacitors. *Electrochim. Acta* **2016**, *191*, 444. [CrossRef]
78. Guo, D.; Zhang, M.; Chen, Z.; Liu, X. Hierarchical Co_3O_4 @PPy Core-Shell Composite Nanowires for Supercapacitors with Enhanced Electrochemical Performance. *Mater. Res. Bull.* **2017**, *96*, 463. [CrossRef]
79. Sulaiman, Y.; Azmi, M.K.S.; Abdah, M.A.A.; Azman, N.H.N. One step electrodeposition of poly-(3,4-ethylenedioxythiophene)/graphene oxide/cobalt oxide ternary nanocomposite for high performance supercapacitor. *Electrochim. Acta* **2017**, *253*, 581. [CrossRef]
80. Yang, P.; Xie, J.; Guo, C.; Li, C.M. Soft- to Network Hard-Material for Constructing Both Ion- and Electron-Conductive Hierarchical Porous Structure to Significantly Boost Energy Density of a Supercapacitor. *J. Colloid Interface Sci.* **2017**, *485*, 137. [CrossRef]
81. Charles, D.S.; Teng, X. Vanadium Pentoxide (V_2O_5) Electrode for Aqueous Energy Storage: Understand Ionic Transport Using Electrochemical, XRay, and Computational Tools. In *Alkali-Ion Batteries*; Yang, D., Ed.; InTechOpen: London, UK, 2016. [CrossRef]
82. Bai, M.-H.; Liu, T.-Y.; Luan, F.; Li, Y.; Liu, X.-X. Electrodeposition of Vanadium Oxide–Polyaniline Composite Nanowire Electrodes for High Energy Density Supercapacitors. *J. Mater. Chem. A* **2014**, *2*, 10882. [CrossRef]
83. Asen, P.; Shahrokhian, S. One Step Electrodeposition of V_2O_5/Polypyrrole/Graphene Oxide Ternary Nanocomposite for Preparation of a High-Performance Supercapacitor. *Int. J. Hydrog. Energy* **2017**, *42*, 21073. [CrossRef]
84. Bi, W.; Wu, Y.; Liu, C.; Wang, J.; Du, Y.; Gao, G.; Wu, G.; Cao, G. Gradient Oxygen Vacancies in V_2O_5 /PEDOT Nanocables for High-Performance Supercapacitors. *ACS Appl. Energy Mater.* **2019**, *2*, 668. [CrossRef]
85. Nithya, V.D.; Arul, N.S. Review on alpha-Fe_2O_3 based negative electrode for high performance supercapacitors. *J. Power Sources* **2016**, *327*, 297. [CrossRef]
86. Ding, Y.; Tang, S.; Han, R.; Zhang, S.; Pan, G.; Meng, X. Iron Oxides Nanobelt Arrays Rooted in Nanoporous Surface of Carbon Tube Textile as Stretchable and Robust Electrodes for Flexible Supercapacitors with Ultrahigh Areal Energy Density and Remarkable Cycling-Stability. *Sci. Rep.* **2020**, *10*, 11023. [CrossRef]
87. Prasanna, B.P.; Avadhani, D.N.; Raghu, M.S.; Yogesh Kumar, K. Synthesis of polyaniline/α-Fe_2O_3 nanocomposite electrode material for supercapacitor applications. *Mater. Today Commun.* **2017**, *12*, 72. [CrossRef]
88. Zhaokun- Yang, Z.; Tang, L.; Ye, J.; Shi, D.; Liu, S.; Chen, M. Hierarchical nanostructured alpha-Fe_2O_3/polyaniline anodes for high performance supercapacitors. *Electrochim. Acta* **2018**, *269*, 21. [CrossRef]
89. Lokhande, V.; Lokhande, A.; Namkoong, G.; Kim, J.H.; Ji, T. Charge Storage in WO_3 Polymorphs and Their Application as Supercapacitor Electrode Material. *Results Phys.* **2019**, *12*, 2012. [CrossRef]
90. Shinde, P.A.; Lokhande, A.C.; Chodankar, N.R.; Patil, A.M.; Kim, J.H.; Lokhande, C.D. Temperature Dependent Surface Morphological Modifications of Hexagonal WO_3 Thin Films for High Performance Supercapacitor Application. *Electrochim. Acta* **2017**, *224*, 397. [CrossRef]
91. Liu, Y.; Jiao, Y.; Zhou, H.; Yu, X.; Qu, F.; Wu, X. Rational Design of WO_3 Nanostructures as the Anode Materials for Lithium-Ion Batteries with Enhanced Electrochemical Performance. *Nano-Micro Lett.* **2015**, *7*, 12. [CrossRef]
92. Yang, F.; Jia, J.; Mi, R.; Liu, X.; Fu, Z.; Wang, C.; Liu, X.; Tang, Y. Fabrication of $WO_3 \cdot 2H_2O$/BC Hybrids by the Radiation Method for Enhanced Performance Supercapacitors. *Front. Chem.* **2018**, *6*, 290. [CrossRef]
93. Das, A.K.; Paria, S.; Maitra, A.; Halder, L.; Bera, A.; Bera, R.; Si, S.K.; De, A.; Ojha, S.; Bera, S.; et al. Highly Rate Capable Nanoflower-like NiSe and WO_3@PPy Composite Electrode Materials toward High Energy Density Flexible All-Solid-State Asymmetric Supercapacitor. *ACS Appl. Electron. Mater.* **2019**, *1*, 977. [CrossRef]
94. Zhuzhelskii, D.V.; Tolstopjatova, E.G. Eliseeva, S.N.; Ivanov, A.V.; Miao, S.; Kondratiev, V.V. PEDOT/WO_3 composite films for high performance supercapacitor application. *Electrochim. Acta* **2019**, *299*, 182. [CrossRef]
95. Samu, G.F.; Pencz, K.; Janaky, C.; Rajeshiwar, K. On the electrochemical synthesis and charge storage properties of WO3/polyaniline hybrid nanostructures. *Electrochim. Acta* **2015**, *19*, 2741. [CrossRef]
96. Ramesh, S.; Yadav, H.M.; Lee, Y.-J.; Hong, G.-W.; Kathalingam, A.; Sivasamy, A.; Kim, H.-S.; Kim, H.S.; Kim, J.-H. Porous Materials of Nitrogen Doped Graphene Oxide@SnO_2 Electrode for Capable Supercapacitor Application. *Sci. Rep.* **2019**, *9*, 12622. [CrossRef]
97. Eedukanti, S.R.; Gampala, A.K.; Rao, K.V.; Chakra, S.; Gedela, V.; Boddula, R. Ultrasonication assisted thermal exfoliation of graphene-tin oxide nanocomposite material for supercapacitor. *Mater. Sci. Energy Technol.* **2019**, *2*, 372. [CrossRef]
98. Hu, Z.-A.; Xie, Y.-L.; Wang, Y.-X.; Mo, L.-P.; Yang, Y.-Y.; Zhang, Z.-Y. Polyaniline/SnO_2 nanocomposite for supercapacitor applications. *Mater. Chem. Phys.* **2009**, *114*, 990. [CrossRef]
99. Wang, L.; Chen, L.; Yan, B.; Wang, C.; Zhu, F.; Jiang, X.; Chao, Y.; Yang, G. In Situ Preparation of SnO_2@polyaniline Nanocomposites and Their Synergetic Structure for High-Performance Supercapacitors. *J. Mater. Chem. A* **2014**, *2*, 8334. [CrossRef]
100. Roy, H.S.; Islam, M.M.; Mollah, M.Y.A.; Susan, M.A.B.H. Polyaniline-MnO_2 Composites Prepared in-Situ during Oxidative Polymerization of Aniline for Supercapacitor Applications. *Mater. Today Proc.* **2020**, *29*, 1013. [CrossRef]

101. Low, W.H.; Khiew, P.S.; Lim, S.S.; Siong, C.W.; Ezeigwe, E.R. Recent Development of Mixed Transition Metal Oxide and Graphene/Mixed Transition Metal Oxide Based Hybrid Nanostructures for Advanced Supercapacitors. *J. Alloys Compd.* **2019**, *775*, 1324. [CrossRef]
102. Liew, S.Y.; Walsh, D.A.; Chen, G.Z. Conducting Polymer Nanocomposites-Based Supercapacitors. In *Conducting Polymer Hybrids*; Springer: Berlin/Heidelberg, Germany, 2017; p. 269. [CrossRef]
103. Okpla, C.C. Nanocomposites An-Overview. *Int. J. Eng. Res.* **2013**, *8*, 17.
104. Yang, D. Application of Nanocomposites for Supercapacitors: Characteristics and Properties. In *Nanocomposites New Trends and Developments*; IntechOpen: London, UK, 2012.
105. Shahabuddin, S.; Gaur, R.; Mukherjee, N.; Chandra, P.; Khanam, R. Conducting polymers-based nanocomposites: Innovative materials for wastewater treatment and energy storage. *Mater. Today Proc.* **2022**, *62*, 6950. [CrossRef]
106. Raza, M.A.; Rehman, Z.U.; Tanvir, M.G.; Maqsood, M.F. Metal oxide-conducting polymer-based composite electrodes for energy storage applications. In *Renewable Polymers and Polymer-Metal Oxide Composites Synthesis, Properties, and Applications*; Haider, S., Haider, A., Eds.; Elsevier: Cambridge, MA, USA, 2022; pp. 195–252.
107. Jadhav, S.A.; Dhas, S.D.; Patil, K.T.; Moholkar, A.V.; Patil, P.S. Polyaniline (PANI)-Manganese Dioxide (MnO_2) Nanocomposites as Efficient Electrode Materials for Supercapacitors. *Chem. Phys. Lett.* **2021**, *778*, 138764. [CrossRef]
108. Zhu, Y.; Xu, H.; Chen, P.; Bao, Y.; Jiang, X.; Chen, Y. Electrochemical performance of polyaniline-coated γ-MnO_2 on carbon cloth as flexible electrode for supercapacitor. *Electrochim. Acta* **2022**, *413*, 140146. [CrossRef]
109. Wei, Y.; Luo, W.; Li, X.; Lin, Z.; Hou, C.; Ma, M.; Ding, J.; Li, T.; Ma, Y. PANI-MnO_2 and Ti_3C_2Tx (MXene) as Electrodes for High-Performance Flexible Asymmetric Supercapacitors. *Electrochim. Acta* **2022**, *406*, 139874. [CrossRef]
110. Zhu, Y.; Xu, H.; Tang, J.; Jiang, X.; Bao, Y.; Chen, Y. Preparation of Ternary Composite CF@γ-MnO_2/PANI Material in Electrochemical Supercapacitors. *J. Mater. Sci. Mater. Electron.* **2021**, *32*, 25300. [CrossRef]
111. Heydari, H.; Abdouss, M.; Mazinani, S.; Bazargan, A.M.; Fatemi, F. Electrochemical Study of Ternary Polyaniline/MoS_2−MnO_2 for Supercapacitor Applications. *J. Energy Storage* **2021**, *40*, 102738. [CrossRef]
112. Ling, X.; Zhang, G.; Long, Z.; Lu, X.; He, Z.; Li, J.; Wang, Y.; Zhang, D. Core-shell structure γ-MnO_2-Pani carbon fiber paper-based flexible electrode material for high performance supercapacitor. *J. Ind. Eng. Chem.* **2021**, *99*, 317. [CrossRef]
113. Poudel, M.B.; Shin, M.; Kim, H.J. Polyaniline-Silver-Manganese Dioxide Nanorod Ternary Composite for Asymmetric Supercapacitor with Remarkable Electrochemical Performance. *Int. J. Hydrog. Energy* **2021**, *46*, 474. [CrossRef]
114. Huang, Y.; Bao, S.; Lu, J. Flower-like MnO_2/Polyaniline/Hollow Mesoporous Silica as Electrode for High-Performance All-Solid-State Supercapacitors. *J. Alloys Compd.* **2020**, *845*, 156192. [CrossRef]
115. Dirican, M.; Yanilmaz, M.; Asiri, A.M.; Zhang, X. Polyaniline/MnO_2/Porous Carbon Nanofiber Electrodes for Supercapacitors. *J. Electroanal. Chem.* **2020**, *861*, 113995. [CrossRef]
116. Bolgam, R.; Boddula, R.; Srinivasan, P. Incorporation of graphene-Mn_3O_4 core into polyaniline shell: Supercapacitor electrode material. *Ionics* **2018**, *24*, 1467–1474. [CrossRef]
117. Naik, Y.V.; Karidurаganavar, M.Y.; Srinivasa, H.T.; Siddagangaiah, P.B. High surface wetting and conducting NiO/PANI nanocomposites as efficient electrode materials for supercapacitors. *Inorg. Chem. Commun.* **2022**, *138*, 109275. [CrossRef]
118. Huang, C.; Hao, C.; Zheng, W.; Zhou, S.; Yang, L.; Wang, X.; Jiang, C.; Zhu, L. Synthesis of Polyaniline/Nickel Oxide/Sulfonated Graphene Ternary Composite for All-Solid-State Asymmetric Supercapacitor. *Appl. Surf. Sci.* **2020**, *505*, 144589. [CrossRef]
119. Kuo, C.-W.; Chang, J.-C.; Wu, B.-W.; Wu, T.-Y. Electrochemical characterization of RuO_2-Ta_2O_5/polyaniline composites as potential redox electrodes for supercapacitor and hydrogen evolution reaction. *Int. J. Hydrog. Energy* **2018**, *45*, 22223. [CrossRef]
120. Arvizu, M.A.; Gonzalez, F.J.; Romero-Galarza, A.; Rodriguez-Varela, F.J.; Garcia, C.R.; Garcia-Lobato, M.A. Symmetric Supercapacitors of PANI Coated RuO_2/TiO_2 Macroporous Structures Prepared by Electrostatic Spray Deposition. *J. Electrochem. Soc.* **2022**, *169*, 020564. [CrossRef]
121. Athira, A.R.; Bhagya, T.C.; Riyas, A.H.; Xavier, T.S.; Shibli, S.M.A. Design and fabrication of Co_3O_4 anchored PANI binary composite supercapacitors with enhanced electrochemical performance and stability. *J. Mater. Sci. Mater. Electron.* **2022**, *33*, 2829. [CrossRef]
122. Fan, Y.; Chen, H.; Li, Y.; Cui, D.; Fan, Z.; Xue, C. PANI-Co_3O_4 with Excellent Specific Capacitance as an Electrode for Supercapacitors. *Ceram Int.* **2021**, *47*, 8433. [CrossRef]
123. Usman, M.; Adnan, N.; Ahsan, M.T.; Javed, S.; Butt, M.S.; Akran, M.A. In Situ Synthesis of a Polyaniline/ Fe-Ni Co-Doped Fe_3O_4 Composite for the Electrode Material of Supercapacitors with Improved Cycling Stability. *ACS Omega* **2021**, *6*, 1190. [CrossRef]
124. Chhetri, K.; Tiwari, A.P.; Dahal, B.; Ojha, G.P.; Mukhiya, T.; Lee, M.; Kim, T.; Chae, S.-H.; Muthurasu, A.; Kim, H.Y. A ZIF-8-Derived Nanoporous Carbon Nanocomposite Wrapped with Co_3O_4-Polyaniline as an Efficient Electrode Material for an Asymmetric Supercapacitor. *J. Electroanal. Chem.* **2020**, *856*, 113670. [CrossRef]
125. Javed, M.S.; Khan, A.J.; Hanif, M.; Nazir, M.T.; Hussain, S.; Saleem, M.; Raza, R.; Yun, S.; Liu, Z. Engineering the Performance of Negative Electrode for Supercapacitor by Polyaniline Coated Fe_3O_4 Nanoparticles Enables High Stability up to 25,000 Cycles. *Int. J. Hydrog. Energy* **2021**, *46*, 9976. [CrossRef]
126. Manna, R.; Srivastava, S.K. Reduced Graphene Oxide/Fe_3O_4 /Polyaniline Ternary Composites as a Superior Microwave Absorber in the Shielding of Electromagnetic Pollution. *ACS Omega* **2021**, *6*, 9164. [CrossRef] [PubMed]

127. Ghebache, Z.; Hamidouche, F.; Safidine, Z.; Trari, M.; Bellal, B. Synthesis and Electrical Conducting Properties of Poly(aniline) Doped with Zeolite HY Nanocomposites Containing SnO_2 for High-Performance Supercapacitor Electrode. *J. Inorg. Organomet. Polym. Mater.* **2019**, *29*, 1548. [CrossRef]
128. Prasanna, B.P.; Avadhani, D.N.; Raj, V.; Kumar, K.Y.; Raghu, M.S. Fabrication of PANI/SnO_2 Hybrid Nanocomposites via Interfacial Polymerization for High Performance Supercapacitors Applications. *Surf. Engin. Appl. Electrochem.* **2019**, *55*, 463. [CrossRef]
129. Bolgam, R.; Boddula, R.; Srinivasan, P. Hybrid Materials of PANI with TiO_2-SnO_2: Pseudocaacitor Electrode for Higher Performance Supercapacitors. *ChemistrySelect* **2017**, *2*, 65. [CrossRef]
130. Wu, X.; Zhang, H.; He, C.; Wu, C.; Huang, K.-J. High-Power-Energy Proton Supercapacitor Based on Interface-Adapted Durable Polyaniline and Hexagonal Tungsten Oxide. *J. Colloid Interface Sci.* **2021**, *601*, 727. [CrossRef]
131. Szkoda, M.; Zarach, Z.; Trzciński, K.; Nowak, A.P. An Aqueous Exfoliation of WO_3 as a Route for Counterions Fabrication—Improved Photocatalytic and Capacitive Properties of Polyaniline/WO_3Composite. *Materials* **2020**, *13*, 5781. [CrossRef]
132. Rehman, M.N.; Munawar, T.; Nadeem, M.S.; Mukhtar, S.; Akbar, U.A.; Manzoor, S.; Hakeem, A.S.; Ashiq, M.N.; Iqbal, F. Facile synthesis of novel PANI covered Y_2O_3–ZnO nanocomposite: A promising electrode material for supercapacitor. *Solid State Sci.* **2022**, *128*, 106883. [CrossRef]
133. Palsaniya, S.; Nemade, H.B.; Dasmahapatra, A.K. Hierarchical PANI-RGO-ZnO Ternary Nanocomposites for Symmetric Tandem Supercapacitor. *J. Phys. Chem. Solids* **2021**, *154*, 110081. [CrossRef]
134. Cao, X.-M.; Han, Z.-B. Hollow core-shell ZnO@ZIF-8 on carbon cloth for flexible supercapacitors with ultrahigh areal capacitance. *Chem. Commun.* **2019**, *55*, 1746. [CrossRef]
135. Gottam, R.; Srinivasan, P. Composite Electrode Material of MoO_3-MC-SiO_2-PANI: Aqueous Supercapacitor Cell with High Energy Density, 1 V and 250,000 CD Cycles. *Polym. Adv. Technol.* **2021**, *32*, 2465. [CrossRef]
136. Bortamuly, R.; Konwar, G.; Boruah, P.K.; Das, M.R.; Mahanta, D.; Saikia, P. CeO_2-PANI-HCl and CeO_2-PANI-PTSA Composites: Synthesis, Characterization, and Utilization as Supercapacitor Electrode Materials. *Ionics* **2020**, *26*, 5747. [CrossRef]
137. Jeyaranjan, A.; Sakthivel, T.S.; Neal, C.J.; Seal, S. Scalable Ternary Hierarchical Microspheres Composed of PANI/ RGO/CeO_2 for High Performance Supercapacitor Applications. *Carbon* **2019**, *151*, 192. [CrossRef]
138. Mahmoud, Z.H.; Adham, R.; Bayati, A.L.; Khadom, A.A. Synthesis and supercapacitor performance of polyaniline-titanium dioxide-samarium oxide (PANI/TiO_2-Sm_2O_3) nanocomposite. *Chem. Pap.* **2022**, *76*, 1401. [CrossRef]
139. Xie, Y.; Zhang, J.; Xu, H.; Zhou, T. Laser-assisted mask-free patterning strategy for high-performance hybrid micro-supercapacitors with 3D current collectors. *Chem. Eng. J.* **2022**, *437*, 135493. [CrossRef]
140. Zhuo, W.-J.; Wang, Y.-H.; Huang, C.-T.; Deng, M.-J. Enhanced Pseudocapacitive Performance of Symmetric Polypyrrole-MnO_2 Electrode and Polymer Gel Electrolyte. *Polymers* **2021**, *13*, 3577. [CrossRef]
141. Pourfarzad, H.; Badrnezhad, R.; Ghaemmaghami, M.; Saremi, M. In situ synthesis of C_3N_4/PPy/MnO_2 nanocomposite as high-performance active material for assymetric supercapacitor. *Ionics* **2021**, *27*, 4057. [CrossRef]
142. Liu, W.; Liu, N.; Shi, Y.; Chen, Y.; Yang, C.; Tao, J.; Wang, S.; Wang, Y.; Su, J.; Li, L.; et al. Wire-Shaped Flexible Asymmetric Supercapacitor Based on Carbon Fiber Coated with Metal Oxide & Polymer. *J. Mater. Chem. A.* **2015**, *3*, 13461. [CrossRef]
143. Kang, C.; Fang, J.; Fu, L.; Li, S.; Liu, Q. Hierarchical Carbon Nanowire/Ni@MnO_2 Nanocomposites for High-Performance Asymmetric Supercapacitors. *Chem. Eur. J.* **2020**, *26*, 16392. [CrossRef] [PubMed]
144. Ates, M.; Kuzgun, O. Modified Carbon Black, CB/MnO_2 and CB/MnO_2 /PPy Nanocomposites Synthesised by Microwave-Assisted Method for Energy Storage Devices with High Electrochemical Performances. *Plast, Rubber Compos.* **2020**, *49*, 342. [CrossRef]
145. Li, X.; Ma, Y.; Shen, P.; Zhang, C.; Cao, M.; Xiao, S.; Yan, J.; Luo, S.; Gao, Y. An Ultrahigh Energy Density Flexible Asymmetric Micro Supercapacitor Based on Ti_3C_2 T_x and PPy/MnO_2 with Wide Voltage Window. *Adv. Mater. Technol.* **2020**, *5*, 2000272. [CrossRef]
146. Ren, C.; Yan, Y.; Sun, B.; Gu, B.; Chou, T.-W. Wet-Spinning Assembly and in Situ Electrodeposition of Carbon Nanotube-Based Composite Fibers for High Energy Density Wire-Shaped Asymmetric Supercapacitor. *J. Colloid Interface Sci.* **2020**, *569*, 298. [CrossRef] [PubMed]
147. Nady, J.E.; Shokry, A.; Khalil, M.; Ebrahim, S.; Elshaer, A.M.; Anas, M. One-step electrodeposition of a polypyrrole/NiO nanocomposite as a supercapacitor electrode. *Sci. Rep.* **2022**, *12*, 3611. [CrossRef] [PubMed]
148. Shen, Z.-M.; Luo, X.-J.; Zhu, Y.-Y.; Liu, Y.-S. Facile Co-Deposition of NiO-CoO-PPy Composite for Asymmetric Supercapacitors. *J. Energy Storage* **2022**, *51*, 104475. [CrossRef]
149. Golkhatmi, S.Z.; Sedghi, A.; Miankushki, H.N.; Khalaj, M. Structural properties and supercapacitive performance evaluation of the nickel oxide/graphene/polypyrrole hybrid ternary nanocomposite in aqueous and organic electrolytes. *Energy* **2021**, *214*, 118950. [CrossRef]
150. Li, S.; Zhang, L.; Zhang, L.; Zhang, J.; Zhou, H.; Chen, X.; Tang, T. The in Situ Construction of Three-Dimensional Core–Shell-Structured TiO_2@PPy/RGO Nanocomposites for Improved Supercapacitor Electrode Performance. *New J. Chem.* **2021**, *45*, 1092. [CrossRef]
151. Xue, J.; Yang, Q.; Guan, R.; Shen, Q.; Liu, X.; Jia, H.; Li, Q. High-Performance Ordered Porous Polypyrrole/ZnO Films with Improved Specific Capacitance for Supercapacitors. *Mater. Chem. Phys.* **2020**, *256*, 123591. [CrossRef]

152. Zhong, M.; Guo, D.; Meng, X.; Bian, L.; Song, Y.; Sun, X.; Liu, X. Heterostructured polypyrrole/hybrid iron oxide composite film as highly stable anode for pseudocapacitors. *J. Power Sources* **2021**, *513*, 230550. [CrossRef]
153. Wang, Y.; Du, Z.; Xiao, J.; Cen, W.; Yuan, S. Polypyrrole-encapsulated Fe_2O_3 nanotube arrays on a carbon cloth support: Achieving synergistic effect for enhanced supercapacitor performance. *Electrochim. Acta* **2021**, *386*, 138486. [CrossRef]
154. Ghanbari, R.; Shabestari, M.E.; Kalali, E.N.; Ghorbani, S.R. Iron (II and III) Oxides/Reduced Graphene Oxide/Polypyrrole Ternary Nanocomposite as Electrochemical Supercapacitor Electrode. *J. Electrochem. Soc.* **2021**, *168*, 030543. [CrossRef]
155. Le, K.; Gao, M.; Xu, D.; Wang, Z.; Wang, G.; Liu, W.; Wang, F.; Liu, J. Polypyrrole- coated Fe_2O_3 constructed by nanoneedles as high-performance anodes for aqueous s asymmetric supercapacitors. *Dalton Trans.* **2020**, *49*, 9701. [CrossRef]
156. Zhuang, Q.; Li, W.; Zhu, Z.; Yu, H.; Chen, W.; Yang, J.; Fu, M. Facile Growth of Hierarchical SnO_2@PPy Composites on Carbon Cloth as All-Solid-State Flexible Supercapacitors. *J. Alloys Compd.* **2022**, *906*, 164275. [CrossRef]
157. Vandana, M.; Nagaraju, Y.S.; Ganesh, H.; Veeresh, S.; Vijeth, H.; Basappaa, M.; Devendrappa, H. A SnO_2QDs/GO/PPY ternary composite film as positive and graphene oxide/charcoal as negative electrodes assembled solid state asymmetric supercapacitor for high energy storage applications. *RSC Adv.* **2021**, *11*, 27801. [CrossRef]
158. Jyothibasu, J.P.; Chen, M.-Z.; Tien, Y.-C.; Kuo, C.-C.; Chen, E.-C.; Lin, Y.-C.; Chiang, T.-C.; Lee, R.-H. V_2O_5/Carbon Nanotube/Polypyrrole Based Freestanding Negative Electrodes for High-Performance Supercapacitors. *Catalysts* **2021**, *11*, 980. [CrossRef]
159. Deng, H.; Huang, J.; Hu, Z.; Chen, X.; Huang, D.; Jin, T. Fabrication of a Three-Dimensionally Networked MoO_3/PPy/RGO Composite for a High-Performance Symmetric Supercapacitor. *ACS Omega* **2021**, *6*, 9426. [CrossRef] [PubMed]
160. Liu, Y.; Ji, X.; Sun, H.; Lin, X. Preparation of Polypyrrole Modified Molybdenum Trioxide Nanorod and Their Applications in Supercapacitors. *Mater. Technol.* **2021**, 1947. [CrossRef]
161. Ramesh, S.; Karuppasamy, K.; Haldorai, Y.; Sivasamy, A.; Kim, H.-S.; Kim, H.S. Hexagonal Nanostructured Cobalt Oxide @ Nitrogen Doped Multiwalled Carbon Nanotubes/Polypyyrole Composite for Supercapacitor and Electrochemical Glucose Sensor. *Colloids Surf. B Biointerfaces* **2021**, *205*, 111840. [CrossRef] [PubMed]
162. Li, W.; Zu, X.; Zeng, Y.; Zhang, L.; Tang, Z.; Yi, G.; Chen, Z.; Lin, W.; Lin, X.; Zhou, H.; et al. Mechanically robust 3D hierarchical electrode via one-step electro-codeposition towards molecular coupling for high-performance flexible supercapacitors. *Nano Energy* **2020**, *67*, 104275. [CrossRef]
163. He, Q.; Ye, J.; Peng, Z.; Guo, Y.; Tan, L.; Chen, Y. Electrodeposition of poly(3,4- ethylenedioxythiophene) coated manganese dioxide nanospheres for flexible asymmetric planar supercapacitor with superior energy density. *J. Power Sources* **2021**, *506*, 230176. [CrossRef]
164. Kim, H.R.; Lee, J.H.; Lee, S.K.; Chun, Y.; Park, C.; Jin, J.-H.; Lee, H.U.; Kim, S.W. Fabricating a modified biochar-based all-solid-state flexible microsupercapacitor using pen lithography. *J. Clean. Prod.* **2021**, *284*, 125449. [CrossRef]
165. Liu, L.; Choi, S. PEDOT: PSS/MnO_2 /CNT Ternary Nanocomposite Anodes for Supercapacitive Energy Storage in Cyanobacterial Biophotovoltaics. *ACS Appl. Energy Mater.* **2020**, *3*, 10224. [CrossRef]
166. Ravit, R.; Azman, N.H.N.; Kulandaivalu, S.; Abdullah, J.; Ahmad, I.; Sulaiman, Y. Cauliflower-like Poly(3,4-ethylenedioxythipohene)/Nanocrystalline Cellulose/Manganese Oxide Ternary Nanocomposite for Supercapacitor. *J. Appl. Polym. Sci.* **2020**, *137*, 49162. [CrossRef]
167. Tatli, S.N.; Unur, E. PEDOT: PSS Enhanced Electrochemical Capacitive Performance of Graphene-Templated delta-MnO_2. *Electrochem. Sci. Technol.* **2020**, *11*, 50. [CrossRef]
168. Jiang, X.; Deng, S.; Liu, J.; Qi, N.; Chen, Z. Metal–Organic Framework Derived NiO/Ni@C Composites as Electrode Materials with Excellent Electrochemical Performance for Supercapacitors. *J. Energy Storage* **2021**, *37*, 102426. [CrossRef]
169. Liu, Y.; Murtaza, I.; Shuja, A.; Meng, H. Interfacial Modification for Heightening the Interaction between PEDOT and Substrate towards Enhanced Flexible Solid Supercapacitor Performance. *Chem. Eng. J.* **2020**, *379*, 122326. [CrossRef]
170. Wang, L.; Shu, T.; Guo, S.; Lu, Y.; Li, M.; Nzabahimana, J.; Hu, X. Fabricating Strongly Coupled V_2O_5@PEDOT Nanobelts/Graphene Hybrid Films with High Areal Capacitance and Facile Transferability for Transparent Solid-State Supercapacitors. *Energy Storage Mater.* **2020**, *27*, 150. [CrossRef]
171. Azman, N.H.N.; Sulaiman, Y. Supercapattery performance of carbon nanofibers decorated with poly(3,4-ethylenedioxythiophene) and cobalt oxide. *Ceram. Int.* **2022**, *48*, 11772. [CrossRef]
172. Zhang, J.; Fan, X.; Meng, X.; Zhou, J.; Wang, M.; Chen, S.; Cao, Y.; Chen, Y.; Bielawski, C.W.; Geng, J. Ice-Templated Large-Scale Preparation of Two-Dimensional Sheets of Conjugated Polymers: Thickness-Independent Flexible Supercapacitance. *ACS Nano* **2021**, *15*, 8870. [CrossRef] [PubMed]
173. Kang, H.; Xu, L.; Cai, Y.; He, Y.; Xu, J.; Zhou, W. Binder-Free and Flexible Carbon- En capsulated Oxygen-Vacancy Cerium Dioxide Electrode for High-Performance Supercapacitor. *J. Electrochim. Soc.* **2021**, *168*, 010536. [CrossRef]
174. Liang, J.; Sheng, H.; Wang, Q.; Yuan, J.; Zhang, X.; Su, Q.; Xie, E.; Lan, W.; Zhang, C.J. PEDOT: PSS-Glued MoO_3 Nanowire Network for All-Solid-State Flexible Transparent Supercapacitors. *Nanoscales Adv.* **2021**, *3*, 3502. [CrossRef] [PubMed]
175. Thakur, A.K.; Choudhary, R.B.; Majumder, M.; Majhi, M. Fairly Improved Pseudocapacitance of PTP/PANI/TiO_2 Nanohybrid Composite Electrode Material for Supercapacitor Applications. *Ionics* **2018**, *24*, 257. [CrossRef]